MANUAL FOR FATIGUE ANALYSIS

OF

REINFORCED CONCRETE STRUCTURAL

ELEMENTS USING

VecTor2

Benard Isojeh

Frank Vecchio

December, 2017

Abstract

The approach for the high-cycle fatigue life prediction of a reinforced concrete structural element using VecTor2 nonlinear finite element analysis is presented. Mechanisms governing fatigue damage progressions are briefly discussed, and the implementation of the models that account for these mechanisms in VecTor2 software is treated subsequently. In addition, an illustrative solution for a single element subjected to shear fatigue loading is given. The VecTor2 nonlinear finite element analysis software, which incorporates fatigue damage models, allows for the prediction of the fatigue residual capacity of an element after a given number of loading cycles. The prediction of the instance at which steel reinforcement will fracture can also be obtained from the analyses results.

Table of contents

List of Figures

CHAPTER 1: FATIGUE DAMAGE MECHANISMS

CHAPTER 2: IMPLEMENTATION OF DAMAGE MODELS IN DSFM

CHAPTER 3: FINITE ELEMENT IMPLEMENTATION

CHAPTER 4: USE OF VecTor2 FOR FATIGUE DAMAGE ANLYSIS

Notation

The following symbols are used (may not be defined in the text):

a,b,c : material parameters

C: material constant = 2 x 10^{-13}

C_f : frequency factor

D : damage

d_{bi}: rebar diameter

D_c: concrete stiffness matrix

D_{cr} : critical damage

D_{ft} : concrete tensile strength damage

D_c: reinforcement stiffness matrix

D_{te} : concrete tensile secant modulus damage

E_c: elastic modulus of concrete

E_{c1}: secant modulus of concrete in tension

E_{c2}: secant modulus of concrete in compression

E_s: elastic modulus of steel reinforcement

G_c: shear modulus

f : frequency

f_{c1}: effective tensile stress of concrete

f_{c2}: effective compressive stress of concrete

$f_{c,TS}$: average tensile stress in concrete due to tension stiffening effect

f_{cx}: normal stress in concrete in horizontal direction

f_{cy}: normal stress in concrete in vertical direction

v_{cxy}: shear stress in concrete in horizontal direction

f_{c2max}: peak compressive stress in concrete considering compression softening effect

f_{eh}: tensile stress due to mechanical anchorage effect of end-hooked steel-fibre

f_f : tensile stress at crack due to steel fibre

f_p : initial compressive strength

f_{st}: tensile stress due to frictional bond behaviour of steel fibre

f_{tp} : initial concrete tensile strength

f'_c: compressive strength of concrete

f_c^*: degraded compressive strength

f_{scri}: local stress in reinforcement at crack

f_{si}: average stress in steel reinforcement

f_t: residual tensile strength of concrete

f_t^*: degraded strength at which concrete cracks

k: post-decay parameter for stress-strain response of concrete in compression

N : number of cycles

n: curve-fitting parameter for stress-strain response of concrete in compression

n: material constant = 3

N_f : numbers of cycles at failure

N_{ij}: interval of cycles considered

s_{cr}: crack spacing

T: period of fatigue cycle

t_d: direction coefficient (= 0.6 or 1.0)

v: Poisson's ratio

v_{ci} : shear stress

$v_{ci,cr}$: shear stress at cracked concrete plane

V_f: steel fibre volume ratio

w_{cr}: crack width

α_{avg} : coefficient to relate tensile stress at a crack due to steel fibres with average tensile stress

α_i: inclination of reinforcement

β : material constant

β_2 : material constant

Δ: deformation

$\Delta\varepsilon_{1cr}$: change in strain at crack

Δf: fatigue stress

δ_s : crack slip

ε_{c1}: net tensile strain

ε_{c2} : net compressive strain

ε^*_c : strain corresponding to the degraded compressive strength

ε_{scri}: local strain in the reinforcement

ε_{si}: average strain in steel reinforcement

ε_d: irreversible fatigue strain

ε_p: initial strain corresponding to the initial compressive strength

ε_{1cr}: local strain at crack

γ_2: parameter for high stress level

γ_s : shear strain due to crack slip

θ, θ_c : inclination of principal strain direction

θ_{ni}: angle between the reinforcement direction and the normal to the crack

ρ_i : reinforcement ratio

CHAPTER 1: FATIGUE DAMAGE MECHANISMS

1.1 Introduction

The fatigue loading of a reinforced concrete element is well-known to result in a progressive deterioration of concrete. Once concrete cracking occurs, reinforcement crack propagation at the intersection with the cracked concrete planes may occur depending on the magnitude of the induced stress in the steel reinforcement. However, robust models required for predicting the fatigue life of these elements are not readily available. This is attributable to the complex degradation mechanisms for steel and concrete composites inherent in any fatigue damage process (Isojeh et al., 2017e).

To fully account for fatigue damage mechanisms, concrete integrity deterioration, irreversible strain accumulation, and reinforcement crack growth should be considered. Herein, the mechanism are incorporated into the constitutive, compatibility and equilibrium equations of the Disturbed Stress Field Model (DSFM) (Vecchio, 2000) analysis algorithm to predict the fatigue residual capacity of a structural element. The fatigue life of a structural element corresponds to the instance when the fatigue residual capacity becomes equal to the applied fatigue load (Isojeh et al., 2017e). The damage mechanisms are considered subsequently.

1.1.1 Strength Degradation

Results of the investigations reported in the literature have shown that concrete strength and stiffness reduce progressively after fatigue loading cycles have been applied (Cook and Chindaprasirt, 1980; Schaff and Davidson, 1997; Edalatmanesh and Newhook, 2013; Isojeh et al., 2017a). To account for this, concrete strength may be modified using a damage factor D_{fc}. Similarly, the stiffness or secant modulus of concrete may be modified using a corresponding

damage factor D_{ce}. Models used for these cases are given thus

$$D = D_{cr} \text{ Exp}\left[s\left(\frac{\Delta f}{f_c'} - u\right)\right] N^v \quad (1.1)$$

$$u = C_f\left(1 - \gamma_2 \log\left(\zeta N_f T\right)\right) \quad (1.2)$$

$$v = 0.434\, s\, C_f\left(\beta_2(1 - R)\right) \quad (1.3)$$

where β_2= 0.0661-0.0226R and γ_2 = 2.47 x 10^{-2}.

ζ is a dimensionless coefficient which is taken as 0.15 for a sinusoidal cycle (Torrenti et al., 2010; Zhang et al., 1998), C_f accounts for the loading frequency, and γ_2 is a constant which accounts for high stress level. From Zhang et al. (1996) on influence of loading frequency,

$$C_f = a b^{-\log f} + c \quad (1.4)$$

where a, b and c are 0.249, 0.920 and 0.796 respectively, and f is the frequency of the fatigue loading. Depending on the value of s estimated from Figure 1.1, D may be taken as D_{fc} or D_{ce}. D_{cr} is a critical damage value taken as 0.35 for concrete strength and 0.4 for fatigue secant modulus (Isojeh et al., 2017a).

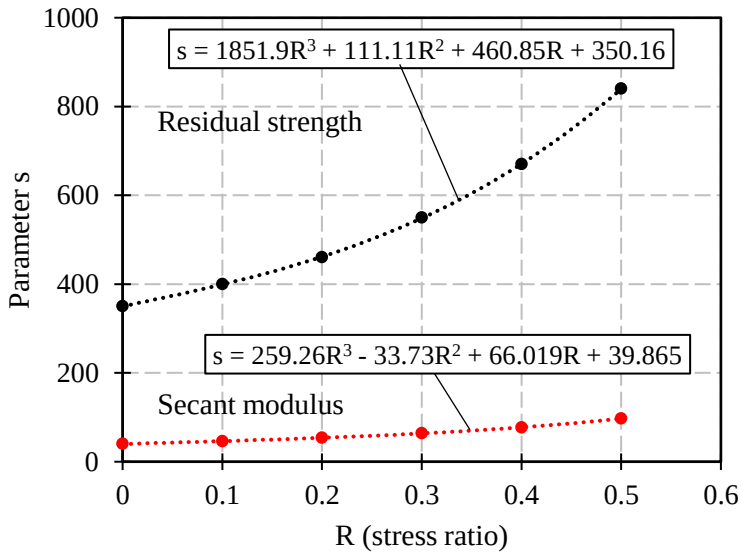

Fig. 1.1 – Estimation of damage parameter s.

1.1.2 Irreversible strain accumulation

Compressive and tensile plastic strains accumulate in concrete under fatigue loading (Holmen, 1982; Gao and Hsu, 1998; Isojeh et al., 2017b). However,the magnitude in tension is usually small, and it is reasonable to assume it to be null. The irreversible compressive strain may be considered as a prestrain and incorporated into the strain compatibility equation. Based on an experimental investigation conducted on the strain evolution of concrete in compression (Isojeh et al., 2017b), models were proposed for the irreversible fatigue strain (ε_d) as follows:

For $0.3N_f \leq N \leq N_f$ (N_f is the number of cycles to failure and N is the fatigue loading cycles)

$$\varepsilon_d = \varepsilon_{do} + \varepsilon_{d1} + \varepsilon_{d2} \tag{1.5}$$

ε_{do} is the strain due to loops centerlines convergence, ε_{d1} is the strain due to the hysteresis loop inclination, and ε_{d2} is the strain due to the minimum stress at the turning point of fatigue loading.

$$\varepsilon_{do} = -\left(\frac{f_c' + (\sigma_{max}\, R)}{E}\right) - 0.3\, \varepsilon_c' \tag{1.6}$$

$$\varepsilon_{d1} = k_2 q \left(\frac{D_{fc}}{\sqrt{D_{ce}}}\right) \tag{1.7}$$

$$\varepsilon_{d2} = \frac{(\sigma_{max}\, R)}{E_{sec}} \tag{1.8}$$

E is the fatigue secant modulus, k_2 is 1.0 for high strength concrete and 2.0 for normal strength concrete, q is equal to $-0.3\, \varepsilon_c'$, R is the stress ratio, σ_{max} is the maximum stress level, and E_{sec} is the static secant modulus at an instance after fatigue loading. The fatigue secant modulus can be taken as $1.5E_{sec}$.

The first stage of deformation under fatigue loading is characterized by cyclic creep. As such, the irreversible strain for any number of cycles less than 30% of the cycles leading to failure (N_f) is

estimated as a function of the irreversible strain at 0.3, where the irreversible strain at 0.3 is estimated using Equations 1.5 to 1.8. Hence, for N < $0.3N_f$,

$$\varepsilon_d = \varepsilon_{d3}\left(\frac{N}{0.3N_f}\right)^{\delta} \tag{1.9}$$

ε_{d3} is the irreversible strain (ε_d) value at $0.3N_f$. The value of δ (fatigue creep constant) can be taken as 0.3. The implementation of the irreversible strain model into constitutive models for normal and high strength concrete are discussed subsequently.

1.1.3 Reinforcement Crack Growth

From the Paris crack growth law (Paris et al., 1961), the propagation of a reinforcing bar crack, up to a depth resulting in fatigue fracture, can be predicted using a parameter representing the stress intensity factor range (ΔK). This parameter is generally expressed as a function of the stress range ($\Delta\sigma$), crack size (a) and a shape factor (Y) for the reinforcing bar (Paris et al., 1961; Rocha and Bruhwiler, 2012; Herwig et al., 2008, Isojeh and Vecchio, 2016). The crack depth (a_y) after a given number of cycles can be estimated as

$$a_y = \left(\frac{{a_i}^{\alpha}}{1-\left[N_{ij}\left(C.\alpha.\pi^{\frac{n}{2}}.Y^n.\Delta\sigma^n.{a_i}^{\alpha}\right)\right]}\right)^{\frac{1}{\alpha}} \tag{1.10}$$

where α = (n/2)-1; C = 2 x 10^{-13}; and n = 3.0 (Hirt and Nussbaumer, 2006).

a_i and a_y are the previous and current crack depth for the interval of cycles considered (N_{ij}), respectively. In order to estimate a_y using Equation 1.10, the value of a_i must be known, which is the previous crack depth (Paris et al., 1961).

An equation for the shape factor (Y) required in Equation 1.10, proposed in BS 7910 (2005) as a function of the crack depth, is given in Equation 1.11.

$$Y = \frac{\frac{1.84}{\pi}\left\{tan\left(\frac{\pi a}{4r}\right)/\left(\frac{\pi a}{4r}\right)\right\}^{0.5}}{cos\left(\frac{\pi a}{4r}\right)} \cdot$$

$$\left[0.75 + 2.02 \cdot \left(\frac{a}{2r}\right) + 0.37 \cdot \left\{1 - sin\left(\frac{\pi a}{4r}\right)\right\}^3\right] \quad (1.11)$$

The initial crack depth (a_i) expressed as a_o at the onset of fatigue loading is obtained iteratively using Equation 1.12:

$$a_o = \frac{1}{\pi}\left(\frac{\Delta K_{th}}{Y\Delta\sigma_{lim}}\right)^2 \quad (1.12)$$

r is the radius of the reinforcing bar, a is the crack depth, $\Delta\sigma_{lim}$ corresponds to the fatigue limit stress at which fatigue damage will not initiate, and ΔK_{th} is the threshold stress intensity factor.

$\Delta\sigma_{lim}$ = 165 - 0.33(R x σ_{max}) (Amir et al., 2012). (1.13)

The crack does not propagate for stress intensity values lower than ΔK_{th}. The ΔK_{th} value is taken as 158 Nmm^2 (Farahmand and Nikbin, 2008) or as a function of the stress ratio R (Dowling, 1993).

ΔK_{th} = 191 N$mm^{-3/2}$ for R ≤ 0.17, or 222.4 (1-0.85R) N$mm^{-3/2}$, for R ≥ 0.17.

where R is the stress ratio ($\sigma_{min}/\sigma_{max}$).

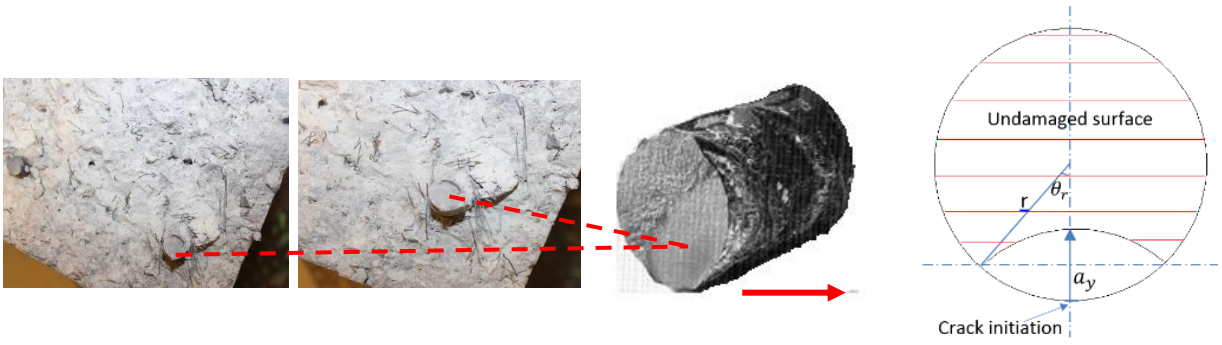

Fig. 1.2 - Crack growth on a reinforcing bar cross section.

The fractured surface area of a reinforcing bar can be assumed as shown in Figure 1.2. The crack depth (a_y) is assumed to evolve from an initiation point up to the instant when the reserve capacity of the reinforcement at the crack is no longer sufficient for tensile stress transfer.

From Figure 1.2, the fractured area (A(a_y)) is estimated as (Isojeh and Vecchio, 2016):

$$\mathrm{A}(a_y) = \frac{\theta_r}{90}\pi r^2 - r sin\theta_r\left(2r - a_y\right) \tag{1.13}$$

$$\theta_r = cos^{-1}\left(\frac{r-0.5a_y}{r}\right) \tag{1.14}$$

The residual area (A_{res}) of a reinforcing bar after crack propagation to a given number of cycles is obtained as:

$$A_{res} = A_o - \mathrm{A}(a_y) \tag{1.15}$$

The reinforcement crack growth factor (Z_O), referred to in other sections as the steel damage parameter, is obtained thus:

$$Z_O = \frac{A_{res}}{A_o} \tag{1.16}$$

where A_o is the cross-sectional area of the uncracked rebar. This is estimated for all reinforcing bars traversing the concrete crack, provided the induced stresses are higher than the threshold value for crack initiation.

Prior to reinforcement crack propagation, the number of cycles resulting in a localised plasticity-crack nucleation or crack initiation may also be included using Masing's model and the SWT approach (Socie et al., 1984; Dowling and Thangjitham, 2000, Isojeh et al., 2017d). To account for this, the value of the reinforcement crack growth factor is assumed to be a value of 1.0 in Equation 1.16 until the estimated crack initiation cycles is reached.

1.2 Damage Constitutive Models for Residual Strength of Concrete

1.2.1 Normal Strength Concrete

The Hognestad stress-strain curve for normal strength is used for estimating the effective stress of a concrete element under a monotonic loading, provided the concrete peak stress (or compressive strength), induced effective strain, and the strain corresponding to the peak stress are

known. Based on the assumption of the intersection of the peak stress of a damaged concrete specimen with the softening portion of the stress-strain envelope (Isojeh et al., 2017b), the Hognestad parabolic equation was modified to obtain the strain corresponding to the degraded strength and, as such, a damage constitutive model was developed for concrete under fatigue loading. This was achieved by modifying the peak strength and the strain corresponding to the peak stress (Figure 1.3). The modification is given thus

$$\left(\frac{\varepsilon_{c2}}{\varepsilon_p}\right)^2 - \frac{2\varepsilon_{c2}}{\varepsilon_p} + \frac{f_{c2}}{f_p} = 0 \qquad (1.17)$$

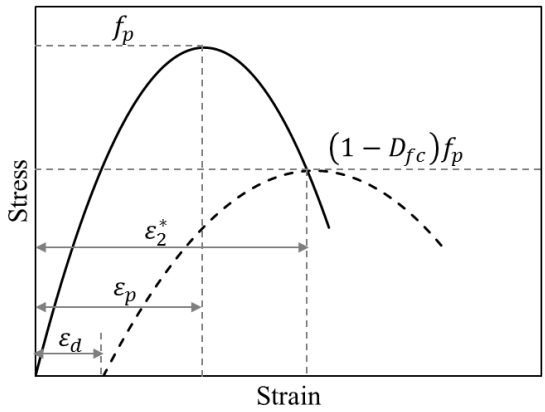

Fig. 1.3 - Modified Stress-strain curve for damaged concrete.

f_{c2} is the principal compressive stress, f_p is the peak concrete compressive stress (equal to f_c') , ε_p (equal to ε_c') is the compressive strain corresponding to f_p, and ε_{c2} is the average net strain in the principal compressive direction.

Based on the assumption $(1 - D_{fc})\, f_p = \mathrm{f_c^*}$, and $f_{c2} = \mathrm{f_c^*}$

$$\left(\frac{\varepsilon_2^*}{\varepsilon_p}\right)^2 - \frac{2\varepsilon_2^*}{\varepsilon_p} + \frac{(1-D_{fc})\, f_p}{f_p} = 0 \qquad (1.18)$$

$$\left(\frac{\varepsilon_2^*}{\varepsilon_p}\right)^2 - \frac{2\varepsilon_2^*}{\varepsilon_p} + (1 - D_{fc}) = 0 \qquad (1.19)$$

$\varepsilon^*{}_2$ is the total strain at peak stress intersection point with stress-strain envelope, and $\mathrm{f_c^*}$ is the

degraded concrete strength. Solving the equation for the total strain corresponding to the new degraded strength gives

$$\varepsilon_2^* = \varepsilon_p \, (1+\sqrt{D_{fc}}) \tag{1.20}$$

From Figure 1.3, it can be observed that the value of ε_2^* also includes the strain offset (ε_d), hence the strain corresponding to the peak stress of the degraded concrete strength ε_c^* is given as:

$$\varepsilon_c^* = \varepsilon_2^* - \varepsilon_d \tag{1.21}$$

$$\varepsilon_c^* = \varepsilon_p \, (1+\sqrt{D_{fc}}) - \varepsilon_d \tag{1.22}$$

where ε_d can be obtained from Equations 1.5 to 1.9, ε_p is equal to the concrete compressive strain corresponding to the peak stress of undamaged concrete, and D_{fc} (concrete strength damage factor) can be estimated as described by Isojeh et al. (2017a) (also given in Equations 1.1 to 1.4).

1.2.2 High Strength Concrete

Popovics stress-strain model was modified for fatigue-damaged concrete for high strength concrete (Isojeh et al., 2017b). The approach is similar to that for normal strength concrete. However, to obtain the strain corresponding to the degraded strength, an iterative method is required such as the Newton-Raphson method. For high strength plain concrete ($f_p \geq 40$ MPa) (using Popovics' equation), the fatigue constitutive equation is given in a simplified form as:

$$f_{c2} = f_p(1 - D_{fc}) \, \frac{n(\varepsilon_{c2}/\varepsilon_p)}{(n-1)+(\varepsilon_{c2}/\varepsilon_p)^{nk}} \tag{1.23}$$

where according to Collins et al. (1997):

$$n = 0.80 - f_p/17 \text{ (in MPa)} \tag{1.24}$$

$$k = 0.6 - \frac{f_p}{62} \qquad for \quad \varepsilon_{c2} < \varepsilon_p < 0 \tag{1.25}$$

$$k = 1 \qquad for \quad \varepsilon_{c2} < \varepsilon_p < 0 \tag{1.26}$$

CHAPTER 2: IMPLEMENTATION OF DAMAGE MODELS IN DSFM

2.1 Disturbed Stress Field Model

The capability of the Disturbed Stress Field Model (Vecchio, 2000; Vecchio, 2001) in predicting the behaviour of reinforced concrete structures subjected to different loading conditions is well documented (Vecchio, 2001; Vecchio et al., 2001; Facconi et al., 2014; Lee et al., 2016). As an extension of the Modified Compression Field Theory (Vecchio and Collins, 1986), the DSFM, founded on a smeared-rotating crack model, includes the consideration of deformation within concrete crack planes. The formulations of the DSFM can be adapted to allow for the consideration of the damage of concrete and the corresponding crack growth on steel reinforcement (longitudinal and transverse) intersecting a concrete crack under fatigue loading. The modification of these models are considered subsequently. The implementation of the fatigue damage mechanisms from Chapter 1 into the equilibrium, compatibility, and constitutive equations are considered herein.

2.1.1 Equilibrium Condition

In Figure 2.1, the normal stresses are denoted by σ_x and σ_y and the shear stress as τ_{xy}. From the average stresses in the element under static loading condition, the equilibrium condition based on the superposition of concrete and steel reinforcement stresses can be expressed as shown in Equations 2.1 to 2.3.

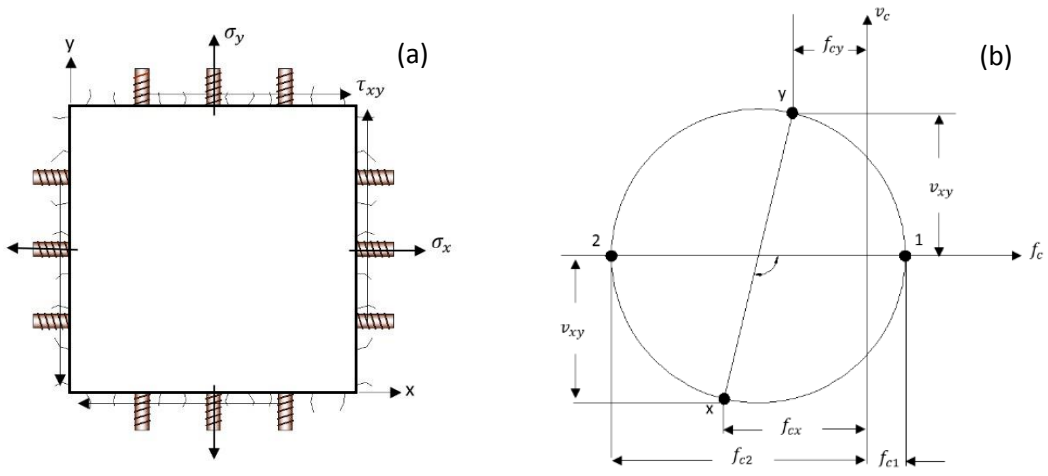

Fig. 2.1 – Reinforced concrete element (a) Loading conditions; (b) Mohr's circle for average stresses in concrete.

$$\sigma_x = f_{cx} + \rho_x f_{sx} \tag{2.1}$$

$$\sigma_y = f_{cy} + \rho_y f_{sy} \tag{2.2}$$

$$\tau_{xy} = v_{cxy} \tag{2.3}$$

where ρ_x and ρ_y are the reinforcement ratios in the x- and y- directions, respectively.

Using Mohr circle (Figure 2.1b), the stresses in the concrete composite (f_{cx}, f_{cy}, and v_{cxy}) can be obtained with known principal stresses (f_{c1}, f_{c2}). The principal stresses are estimated from constitutive models which are functions of concrete strength, stiffness, and induced strains. As a result of fatigue loading, these parameters (strength and stiffness) degrade and strains accumulate; hence, the material stresses change correspondingly.

2.1.1.1 Equilibrium of Stresses at a Crack

Under static loading, stresses in the reinforcement at crack locations are higher than the values between cracks (average values) since the concrete tensile stress is zero at such locations. As a

result, shear stresses also develop on the surfaces at crack locations.

Since fatigue crack propagation is a function of the stress values, its initiation tends to occur at a reinforcement region traversing the concrete cracks where the stresses are high. From Figures 2.2(a) and 2.2(b), the general static equilibrium equations which involves steel fibre are given thus (Lee et al., 2016)

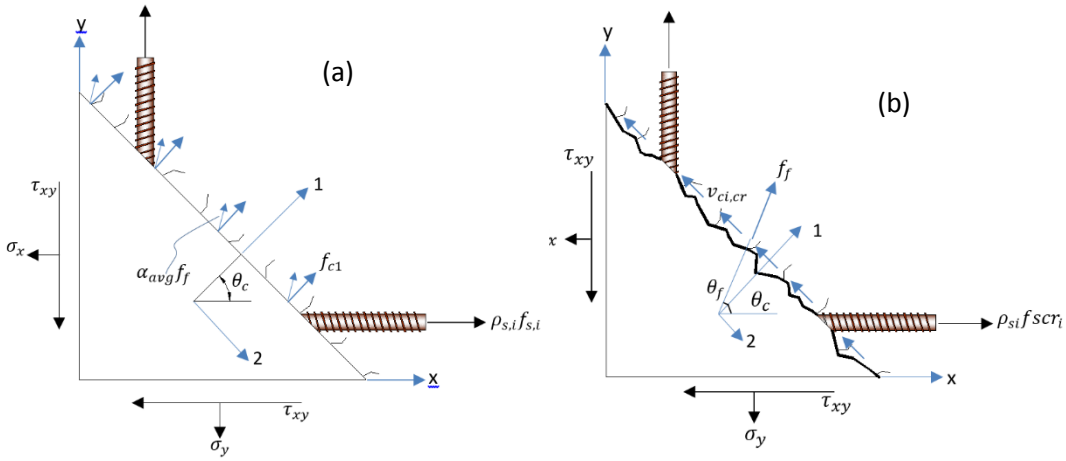

Fig. 2.2 - Equilibrium conditions: (a) Parallel to crack direction; (b) Along crack surface.

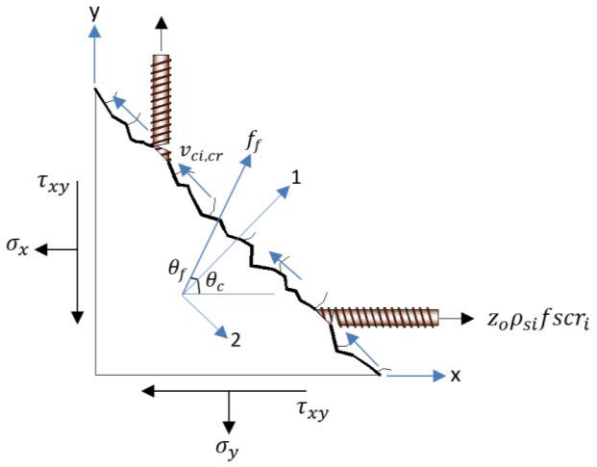

Fig. 2.3 - Equilibrium conditions along crack surface after reinforcement crack propagation.

$$f_{c1} = \sum_i^n \rho_{si}(f_{scri} - f_{si}).\ cos^2\theta_{ni} + (1-\alpha_{avg}) f_f cos\theta_f \quad (2.4)$$

$$v_{ci,cr} = \sum_i^n \rho_{si}(f_{scri} - f_{si}).\ cos\theta_{ni}\ sin\theta_{ni} - (1-\alpha_{avg}) f_f\ sin\theta_f \quad (2.5)$$

In Equations 2.4 and 2.5, (1-α_{avg})f_f represents the contribution from steel fibre bridging a crack. α_{avg} relates the tensile stress in steel fibre to the average principal tensile stress, while f_f is a function of the equivalent bond strength due to the mechanical anchorage of the steel fibre and the friction bond strength of steel fibre (Lee et al., 2016).

As cracks propagate in the reinforcement traversing a concrete crack, the area of reinforcement intersecting the crack reduces, hence resulting in lower reinforcement ratio at the crack region. To account for the progressive reinforcement ratio reduction due to fatigue loading, Equations 2.4 and 2.5 are modified thus (Figure 2.3):

$$f_{c1} = \sum_i^n \rho_{si}(Z_O f_{scri} - f_{si}).\ cos^2\theta_{ni} \ + (1-\alpha_{avg}) f_f \sqrt{1 - D_{fc}}\ cos\theta_f \quad (2.6)$$

$$v_{ci,cr} = \sum_i^n \rho_{si}(Z_O f_{scri} - f_{si}).\ cos\theta_{ni}\ sin\theta_{ni} - (1-\alpha_{avg}) f_f \sqrt{1 - D_{fc}}\ sin\theta_f \quad (2.7)$$

Z_O and D_{fc} are parameters representing reinforcement crack growth and plain or steel fibre concrete strength degradation, respectively.

2.1.2 Compatibility Condition

In the Disturbed Stress Field Model, the total strain $[\varepsilon]$ in an element comprises of the net strain $[\varepsilon_c]$, plastic offset strain $\left[\varepsilon_c^p\right]$, elastic offset strain $[\varepsilon_c^o]$, and strain effect due to slip at crack $[\varepsilon_c^s]$. As indicated in Chapter 1, the irreversible strain is also considered as a prestrain (ε_d or $\left[\varepsilon_{c,2}^{fat}\right]$).

In the x-y direction, the total strain $[\varepsilon]$ is

$$[\varepsilon] = [\varepsilon_c] + \left[\varepsilon_c^p\right] + [\varepsilon_c^o] + [\varepsilon_c^s] + \left[\varepsilon_c^{fat}\right] \quad (2.8)$$

$$[\varepsilon] = \left[\varepsilon_x, \varepsilon_y, \gamma_x\right] \quad (2.9)$$

$$[\varepsilon_c] = [\varepsilon_{cx}, \varepsilon_{cy}, \gamma_{cx}] \quad (2.10)$$

$$[\varepsilon_c^{fat}] = [\varepsilon_{cx}^{fat}, \varepsilon_{cy}^{fat}, \gamma_{cxy}^{fat}] \quad (2.11)$$

From a strain transformation of the fatigue prestrain,

$$\varepsilon_{cx}^{fat} = \frac{1}{2}\varepsilon_{c,2}^{fat}(1 - \cos 2\theta) \quad (2.12)$$

$$\varepsilon_{cy}^{fat} = \frac{1}{2}\varepsilon_{c,2}^{fat}(1 + \cos 2\theta) \quad (2.13)$$

$$\gamma_{cxy}^{fat} = \varepsilon_{c,2}^{fat} \sin 2\theta \quad (2.14)$$

From Mohr's circle of strain, the principal strains from the net strains can be estimated as:

$$\varepsilon_{c1}, \varepsilon_{c2} = \frac{(\varepsilon_{cx}+\varepsilon_{cy})}{2} \pm \frac{1}{2}\left[(\varepsilon_{cx} - \varepsilon_{cy})^2 + \gamma_{cx}{}^2\right]^{1/2} \quad (2.15)$$

The inclination of the principal strains in the concrete, θ, is given by:

$$\theta = \frac{1}{2} tan^{-1}\left[\frac{\gamma_{cx}}{\varepsilon_{cx}-\varepsilon_{cy}}\right] \quad (2.16)$$

2.1.3 Constitutive Relation

2.1.3.1 Concrete Constitutive Model

The behaviour of cracked concrete in compression and the corresponding influences of transverse stresses and shear slip effects under static loading are well illustrated in Vecchio (2000). Constitutive models for plain and steel fibre reinforced concrete are usually given in terms of peak stresses and the corresponding strains at peak stresses. Fatigue constitutive models for plain concrete have been described in Chapter 1. Depending on the steel fibre volume ratio in concrete, the damage parameter s required in the damage model in Chapter 1 may also be obtained from Figure 2.4.

For steel fibre concrete, the monotonic constitutive model proposed by Lee et al. (2016) was simply modified to account for fatigue damage; thus:

$$f_{c2} = f_{c2max}\left(1 - D_{fc}\right)\left[\frac{A(\varepsilon_{c2}/\varepsilon_{\mathrm{p}})}{A-1+(\varepsilon_{c2}/\varepsilon_{\mathrm{p}})^{B}}\right] \tag{2.17}$$

where:

$$f_{c2max} = \frac{f_c'}{1+0.19(-\varepsilon_{c1}/\varepsilon_{c2}-0.28)^{0.8}} \quad \not> f_c' \tag{2.18}$$

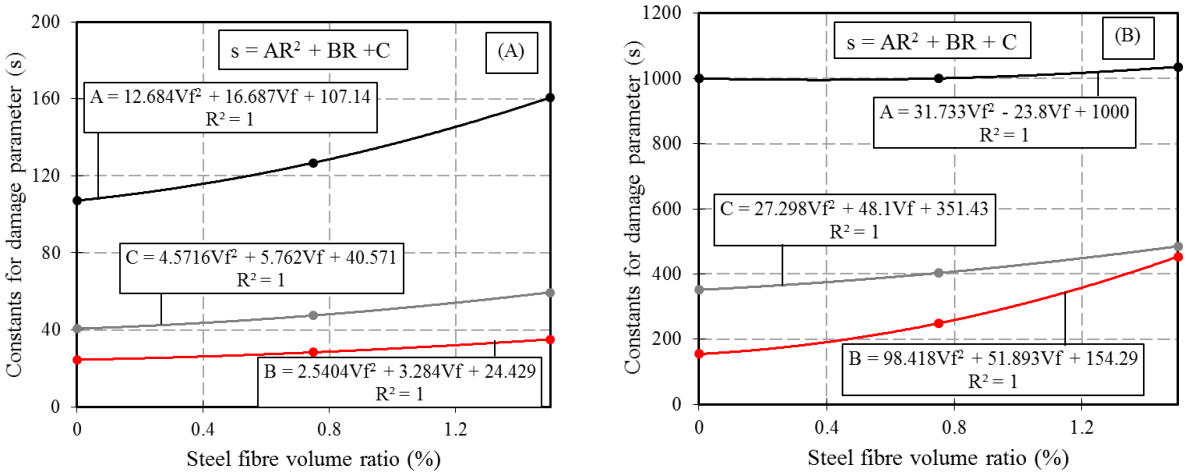

Fig. 2.4 - Damage parameter s for steel fibre secant modulus (A) and residual strength (B).

The values for A and B in Equation 2.17 differ for the hardening and softening portion of the stress-strain envelope. From Lee et al. (2016), the values are given thus:

For the pre-peak ascending branch,

$$A = B = 1/[1-(f_c'/\varepsilon_c' E_c) \tag{2.19}$$

For the post-peak descending branch,

$$A = 1 + 0.723(V_f l_f/d_f)^{-0.957};\ B = (f_c'/50)^{0.064}[1 + 0.882\ (V_f l_f/d_f)^{-0.882}] \tag{2.20}$$

The behaviour of cracked concrete has been considered so far. In an uncracked element, a linear relation for concrete in tension is modified. Thus

$$f_{c1} = E_c(1 - D_{te})\varepsilon_{c1} \tag{2.21}$$

where E_c is the initial tangential modulus, and ε_{c1} is the principal tensile strain in the concrete. Compressive fatigue damage in an uncracked concrete element is generally considered

insignificant, since the induced compressive stress is usually small. D_{te} is the damage of concrete stiffness in tension using Equations 1.1 to 1.4 in Chapter 1. However, tensile stresses are used in the models.

Under fatigue loading, the effect of tension stiffening reduces progressively due to the evolving tensile strain in cracked concrete and reinforcement crack propagation. The coefficient c_f in Equation 2.22 accounts for the influence of steel fibre (end-hooked),

$$f_{c,TS} = \frac{f_{tp}}{1+\sqrt{3.6 c_f . \varepsilon_{c1}}} \tag{2.22}$$

c_f= 0.6 + (1/0.034) (l_f/d_f)[$\left(100V_f\right)^{1.5}/M^{0.8}$]; M (bond parameter) = A_c/ ($\sum d_{bs}\pi$), in millimeters.

For plain concrete, the value of c_f reduces to 0.6. The tensile stress in steel fibre concrete is estimated as the sum of the tension stiffening effect and the stresses transmitted by steel fibre across cracks; hence,

$$f_{c1} = f_{c,TS} + (1-\alpha_{avg}) f_f \cos\theta_f \tag{2.23}$$

where f_{c1} is the effective tensile stress in the concrete, ε_{c1} is the tensile strain of the concrete, d_{bi} is the rebar diameter, θ is the inclination of principal strain direction, α_i is the inclination of reinforcement, and *n* is the number of reinforcement directions. The second term in Equation 2.23 is zero in the case of conventional reinforced concrete.

The tensile stress in Equation 2.23 is required to be less or equal to the right-side of Equation 2.6. Further, the crack spacing model proposed by Deluce et al. (2014) is used to relate crack width to average tensile strain, while the shear slip model proposed by Vecchio and Lai (2004) is used to estimate the slip prestrain and deviation of steel fibre tensile stress. The models are given subsequently:

For steel fibre concrete,

$$S_{cr} \text{ (average crack spacing)} = 2\left(c_a + \frac{s_b}{10}\right) k_3 + \frac{k_1 k_2}{s_{mi}} \quad (2.24)$$

where $c_a = 1.5a_{gg}$; $k_1 = 0.4$; $k_2 = 0.25$; $k_3 = 1 - [\min(V_f, 0.015)/0.015][1-(1/k_f)]$;

a_{gg} is the maximum aggregate size, given in millimeters.

$$s_b = \frac{1}{\sqrt{\sum_i \frac{4\rho_{s,i}}{\pi d_{b,i}^2} cos^4\theta_i}} \quad (2.25)$$

$$s_{m,i} = \sum_i \frac{\rho_{s,i}}{d_{b,i}} cos^2\theta_i + k_f \frac{\alpha_f V_f}{d_f} \quad (2.26)$$

For conventional reinforced concrete, $S_{cr} = \frac{1}{|cos\theta|/s_{mx} + |sin\theta|/s_{my}}$

$$\delta_s \text{ (crack slip)} = \delta_2 \sqrt{\frac{\psi}{1-\psi}} \quad (2.27)$$

$$\delta_2 = \frac{0.5v_{cmax} + v_{co}}{1.8w_{cr}^{-0.8} + (0.234w_{cr}^{-0.707} - 0.20)f_{cc}} \quad (2.28)$$

$\psi = v_{ci,cr}/v_{cmax}$; v_{cmax} (in MPa) = $\sqrt{f_c'}$/ [0.31 + ($24\frac{w_{cr}}{a_{gg}} + 16$); $v_{co} = f_{cc}/30$; f_{cc} (in MPa), is taken as the concrete cube strength; $w_{cr} = S_{cr}\varepsilon_{c1}$. For conventional reinforced concrete, δ_s is taken as δ_2, but the numerator is replaced with the shear stress v_{ci} (Equation 2.27).

The shear strain resulting from the crack slip is estimated as $\gamma_s = \delta_s/s$; and resolving into x and y components,

$$\varepsilon_x^s = -\gamma_s/2.\ \sin 2\theta \quad (2.29)$$

$$\varepsilon_y^s = \gamma_s/2.\ \sin 2\theta \quad (2.30)$$

$$\gamma_{xy}^s = -\gamma_s/2.\ \cos 2\theta \quad (2.31)$$

Since the shear stresses and slip are functions of the reinforcement ratio or progressing principal stresses, their values also evolve under fatigue loading. The tensile stress resulting from steel fibre

bridging deviates by an angle θ_f from the direction of the principal tensile stress (f_{c1}). This deviation angle, according to Lee et al. (2016), is estimated thus:

$$\theta_f = tan^{-1} \frac{\delta_s}{w_{cr}} \tag{2.32}$$

2.1.3.2 Conventional Reinforcement

Although a trilinear stress-strain relation is used to model the response of reinforcement in the Disturbed Stress Field Model, a bilinear stress-strain relation (elastic-perfectly plastic) is used for fatigue analysis. This is attributed to the fact that the behaviour of reinforcement under high cycle fatigue loading is usually brittle; hence increased strength due to strain hardening is avoided.

CHAPTER 3: FINITE ELEMENT IMPLEMENTATION

3.1 Formulation

The general formulation of material stiffness matrix is expressed thus:

$$[\sigma] = [\mathrm{D}]\,[\varepsilon] - [\sigma^o] \tag{3.1}$$

$\{\sigma\}$ and $\{\varepsilon\}$ are the total stress and total strain vectors due to the applied maximum fatigue load. (The ratio of the minimum to maximum fatigue loading is a parameter R required in a subsequent section.) $[D]$ is the transformed composite stiffness matrix in which the concrete composite degrades progressively due to fatigue loading.

$$\{\sigma\} = \begin{bmatrix} \sigma_x \\ \sigma_y \\ \tau_{xy} \end{bmatrix} \text{ (normal and shear stresses on an element)} \tag{3.2}$$

$$\{\varepsilon\} = \begin{bmatrix} \varepsilon_x \\ \varepsilon_y \\ \gamma_{xy} \end{bmatrix} \text{ (corresponding strain values)} \tag{3.3}$$

$$[D] = [D_c\,] + \sum_{i=1}^{n} [D_s]_i + [D_f\,] \tag{3.4}$$

Prior to cracking,

$$[D_c] = \frac{E_c\,(1-D_{te})}{1-\mathrm{v}^2} \begin{bmatrix} 1 & \frac{\mathrm{v}}{(1-D_{te})} & 0 \\ \mathrm{v} & \frac{1}{(1-D_{te})} & 0 \\ 0 & 0 & \frac{1-\mathrm{v}}{2(1-D_{te})} \end{bmatrix} \tag{3.5}$$

As previously indicated, D_{te} may be obtained using Equations 1.1 to 1.4 in Chapter 1. However, Δf and f_c' are replaced with the induced tensile stress and the concrete tensile strength of concrete, respectively. For a given element strain condition, normal stresses in the concrete may be found and subsequently, the principal tensile and compressive stresses and the principal strain direction obtained.

For a two-dimensional cracked state, the stiffness of the concrete with respect to the axes of orthotrophy, the stiffness of the steel reinforcement with respect to its direction, and the stiffness of the steel fibre with respect to the inclination of tensile stress due to steel fibre are all required (Equations 3.6 to 3.8). Subsequently, the stiffnesses are transformed back to the reference x, y axes (Equations 3.9 and 3.10).

$$[D_c]' = \begin{bmatrix} \overline{E_{c1}} & 0 & 0 \\ 0 & \overline{E_{c2}} & 0 \\ 0 & 0 & \overline{G_c} \end{bmatrix} \text{ for concrete} \quad (3.6)$$

$\overline{E_{c1}} = f_{c1}/\varepsilon_{c1}$; $\overline{E_{c2}} = f_{c2}/\varepsilon_{c2}$; and $\overline{G_c} = \overline{E_{c1}}.\ \overline{E_{c2}}/\ (\overline{E_{c1}} + \overline{E_{c2}})$

$$[D_s]_i' = \begin{bmatrix} \rho_i\overline{E_{s\iota}} & 0 & 0 \\ 0 & 0 & 0 \\ 0 & 0 & 0 \end{bmatrix} \text{ for steel reinforcement} \quad (3.7)$$

$\overline{E_{s\iota}} = f_{s,i}/\varepsilon_{s,i}$

$$[D_f]' = \begin{bmatrix} \rho_i\overline{E_{f1}} & 0 & 0 \\ 0 & 0 & 0 \\ 0 & 0 & 0 \end{bmatrix} \text{ for steel fibre} \quad (3.8)$$

$\overline{E_{f1}} = \alpha_{avg} f_f/\varepsilon_{cf}$; $\varepsilon_{cf} = (\varepsilon_{c1} + \varepsilon_{c2})/2 + [(\varepsilon_{c1} - \varepsilon_{c2})/2]\cos 2\theta_f$

$[D_c\,] = [T_c]^T [D_c]' [T_c\,]$; $[D_f\,] = [T_f]^T [D_f]' [T_f\,]$;

$$[D_{s,i}\,] = [T_{s,i}]^T [D_{s,i}]' [T_{s,i}\,] \quad (3.9)$$

$$[T] = \begin{bmatrix} cos^2\psi & sin^2\psi & cos\psi sin\psi \\ sin^2\psi & cos^2\psi & -cos\psi sin\psi \\ -2cos\psi sin\psi & 2cos\psi sin\psi & (cos^2\psi - sin^2\psi\,) \end{bmatrix} \quad (3.10)$$

For concrete, $\psi = \theta_c$, for steel fibre, $\psi = \theta_c + \theta_f$, and for a steel reinforcing bar, $\psi = \alpha_i$.

σ^o (Equation 3.11) is estimated as a pseudo-load using Equations 2.8 to 2.16 in Chapter 2. For a given stress condition and loading cycle (due to applied fatigue load), the total strain in the element

can be obtained. The solution approach is iterative since the secant moduli of materials are needed to find the strain condition $\{\varepsilon\}$ and vice versa.

$$[\sigma^o] = [D_c\,]\,(\left[\varepsilon_c^p\right] + [\varepsilon_c^o] + [\varepsilon_c^s] + \left[\varepsilon_c^{fat}\right]) \tag{3.11}$$

In the iterative process for an element at the first fatigue loading cycle, strain values are initially assumed. Subsequently, the principal strain values and the corresponding inclination of the principal tensile strain are estimated. Using the modified compatibility and constitutive equations illustrated previously, the net strains are estimated and subsequently, the average principal stresses in the concrete and the average stresses in the reinforcement are obtained with the assumption that fatigue damage is zero.

Stresses at the crack are also checked and shear stress and crack slip are estimated using the modified equilibrium equation; however, Z_o is assumed to be zero for the first cycle. From the crack slip, prestrains are estimated and are subtracted from the total strains in order to obtain net strains. Further, secant moduli for the constituent materials are estimated and the material stiffness matrices are obtained using Equations 3.7 to 3.10. Subsequently, the total strains are obtained and compared with the previous values assumed (Equation 3.12). The iterative process continues until the errors become minimal. The element stresses estimated are saved for subsequent loading cycles.

$$[\varepsilon] = [\mathrm{D}]^{-1}\,([\sigma] + [\sigma^o]) \tag{3.12}$$

For subsequent fatigue loading cycles, the saved stresses and the number of fatigue loading cycles considered are substituted into the corresponding fatigue damage model (described in Chapter 1) to estimate the required damage for the irreversible strain, the modified constitutive models, and the modified equilibrium equations. The described iterative process is also repeated as the fatigue

loading cycles are increased. Failure becomes imminent when instability due to fractured reinforcement or significant crushing of concrete occurs. Deformation evolution plots can be obtained from the material parameter values as the fatigue loading cycles are increased up to the point of failure.

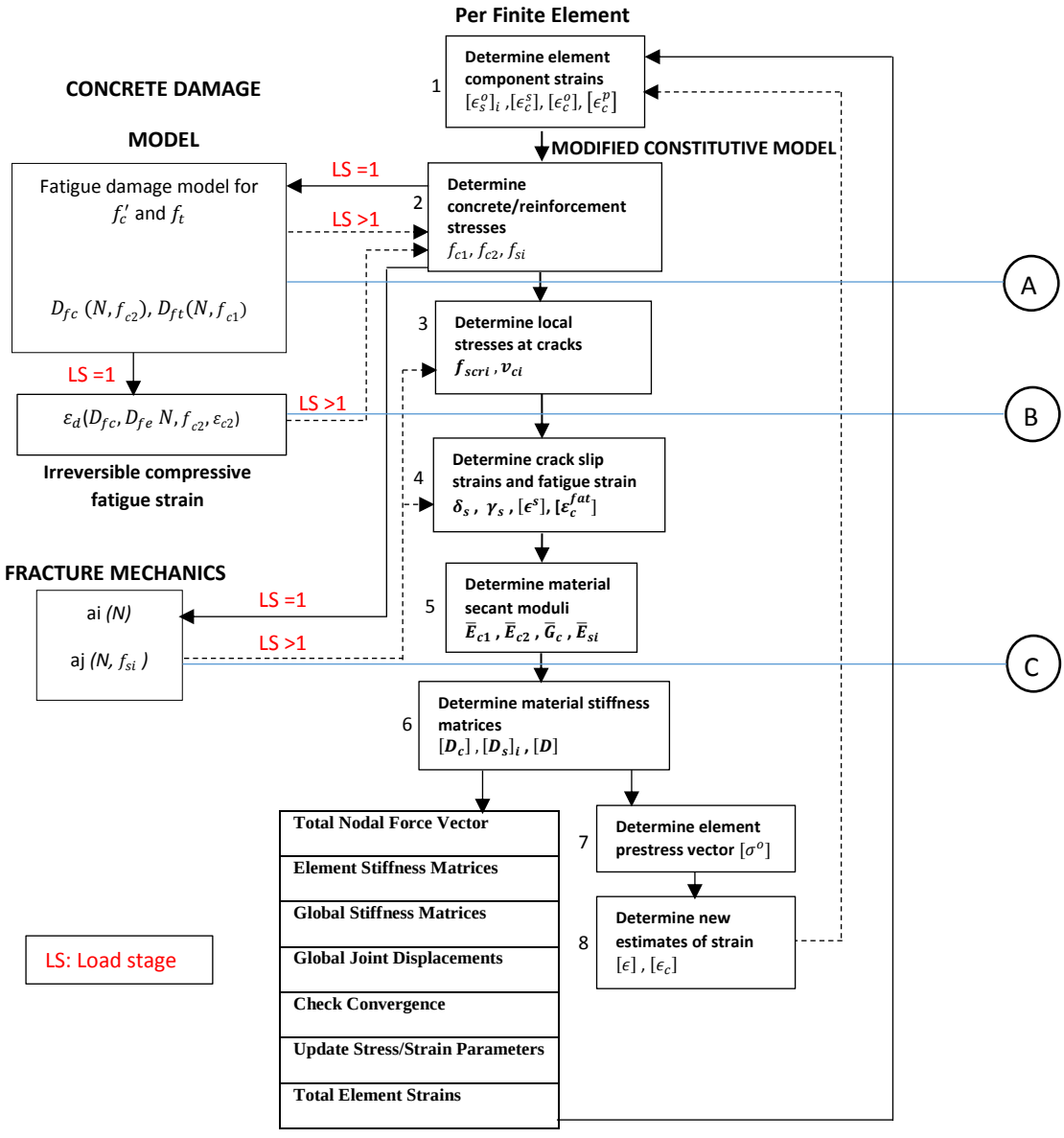

Fig. 3.1 - Flow chart for the modified solution algorithm for DSFM.

The modified algorithm for the Disturbed Stress Field Model which accounts for fatigue damage in an element is shown in the flow chart in Figure 3.1. The original algorithm is void of the damage models (A, B, and C). In all, the analyses involve modelling the monotonic loading responses of structural components which exhibit some level of damage due to fatigue loading cycles.

3.2 Failure Criterion for Reinforced Concrete and Steel-Fibre Concrete under Fatigue Loading

The evolution of deformation is attributed to plain or steel fibre concrete strength and stiffness deterioration, irreversible strain accumulation, and steel reinforcement crack growth (A, B, and C in Figure 3.1). Monotonic tests of structural elements subjected to different fatigue loading cycles will exhibit decreasing resistance capacity as the loading cycles increase. The number of cycles at which the residual capacity of the element becomes equal to the fatigue load is termed the fatigue life of the structural element. At this instant, severe crushing of concrete or fracture of reinforcing bars may occur, leading to structural collapse.

For further exemplification, the solution to the fatigue analysis of a shear panel is illustrated using the flow chart given in Figure 3.1 in a stepwise manner. The properties and loading parameters are also given. Three different pure shear fatigue loads (Figure 3.2) (3.5 MPa, 3.0 MPa, and 2.7 MPa) were used and the corresponding deformation evolution of the material parameters were obtained. The significance of the proposed analysis approach can be observed from the predicted three-staged deformation evolution plots. In addition, the effect of fatigue loading is explicitly shown in all plots given in Figures 3.3 to 3.8.

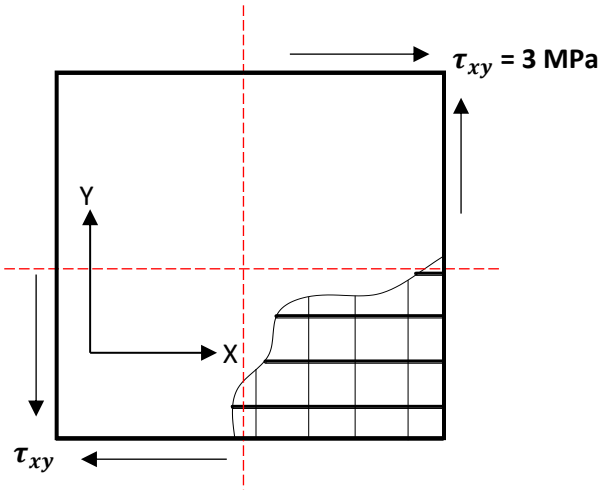

Fig. 3.2 - Shear panel (PV19).

f_c' = 19.0 MPa; ρ_x = 1.785%

f_t' = 1.72 MPa; ρ_y = 0.713%

ε_c' = -2.15 x 10^{-3}; f_{yx} = 458 MPa

f_{yy} = 300 MPa

E_s = 200000 MPa

a = 10 mm

$s_x \approx$ 50 mm $d_{bx} \approx$ 6.35 mm

$s_y \approx$ 50 mm $d_{by} \approx$ 4.01 mm

Fatigue frequency = 5 Hz waveform = sinusoidal

Load ratio (R) = 0

$$[\sigma] = \begin{bmatrix} 0 \\ 0 \\ 3.0 \end{bmatrix} \text{ MPa}$$

Solution:

The assumed initial total and net strains (from previous calculations) for an applied shear stress of 3.0 MPa on the shear element in Figure 3.2, are:

$$\{\varepsilon\} = \begin{bmatrix} 0.431 \\ 0.792 \\ 1.725 \end{bmatrix} \text{ x } 10^{-3} \qquad \{\varepsilon_c\} = \begin{bmatrix} 0.566 \\ 0.659 \\ 1.716 \end{bmatrix} \text{ x } 10^{-3}$$

Using the iterative process described previously, the monotonic response of the shear panel which includes induced stress and strain values due to the applied fatigue load (3.0 MPa) is obtained (without considering fatigue damage). The obtained and saved element stresses due to the monotonic response or at the first cycle, required in calculating damage values in subsequent cycles, are given thus:

f_{sx} = 111 MPa; f_{sy} = 241 MPa (both stresses are required in the fracture mechanics model)

f_{c2} = -5.35 MPa; f_{c1} = 1.08 MPa (required in concrete damage model and irreversible strain model).

These values are substituted into A, B, and C in Figure 3.1 to estimate the corresponding damage at any given fatigue loading cycle. Having accounted for the corresponding damage, the monotonic response is again obtained iteratively. This is repeated for given cycles until instability is reached.

3.3 Solution for Fatigue Loading at 10000 cycles

Figure 3.1 (Box 1) - Strain components after iterations are:

$$\{\varepsilon\} = \begin{bmatrix} 0.584 \\ 1.278 \\ 2.604 \end{bmatrix} \text{ x } 10^{-3} \qquad \{\varepsilon_c\} = \begin{bmatrix} 0.804 \\ 1.072 \\ 2.569 \end{bmatrix} \text{ x } 10^{-3}$$

The principal strains are estimated from $\{\varepsilon_c\}$ (Equations 2.15 and 2.16 in Chapter 2) as:

$$\varepsilon_{c1} = 2.23 \text{ x } 10^{-3} \qquad \varepsilon_{c2} = -0.353 \text{ x } 10^{-3} \qquad \theta_\sigma = 42.02^0$$

Figure 3.1 (Box 2) - Average Stresses in Concrete and Reinforcement:

Since the concrete is in a cracked state, Equations 1.18 to 1.19 in Chapter 1 are used for concrete compressive stress. The damage parameter required in the equation is obtained from Equations 1.1 to 1.3. The fatigue prestrain value (Equation 2.12 to 2.14) is also required in estimating the concrete compressive stress.

f_{c2} = 5.34 MPa

f_{c1} = 1.07 MPa

Assuming perfect bond between the concrete and the steel reinforcement, the average strain in the concrete is equal to the average strain in the steel reinforcing bars. Hence:

E_s = 200000 MPa

ε_{sx} = 0.584 x 10^{-3}

ε_{sy} = 1.278 x 10^{-3}

$f_{sx} = E_s\ \varepsilon_{sx}$ = 117 MPa (x-direction)

$f_{sy} = E_s\ \varepsilon_{sy}$ = 256 MPa (Y-direction)

Figure 3.1 (Box 3) - Local stresses at crack:

The local stresses are estimated from Equations 2.6 and 2.7 (neglecting the influence of steel fibre). In Equations 2.6 and 2.7, the reinforcement crack growth factor (Z_o) is estimated from Equations 1.10 to 1.16 (shown as C in Figure 3.1). The average reinforcement stresses are required in C in order to estimate the progressive crack depth; Thus:

ε_{scrx} = 1.033 x 10^{-3} , f_{scrx} = 207 MPa

ε_{scry} = 1.642 x 10^{-3} , f_{scry} = 300 MPa

v_{ci} = 0.621 MPa

Figure 3.1 (Box 4) - Crack slip strains:

The slip at a given fatigue loading cycle can be estimated using Equation 2.27. Subsequently, the shear strains (in x-y directions) resulting from slip at the crack are estimated. Fatigue irreversible compressive strain values are also estimated in the x-y direction (Equations 2.12 to 2.14). The prestrain is equal to the summation of the shear strains. The pseudo-load [σ^o] is estimated from the obtained values of prestrain.

The shear strain resulting from the crack slip is estimated as: $\gamma_s = \delta_s/s$ = 0.429 x 10^{-3}; resolving into x and y components,

$$\varepsilon_x^s = -\gamma_s/2.\ \sin 2\theta = -0.213 \times 10^{-3}$$

$$\varepsilon_y^s = \gamma_s/2.\ \sin 2\theta = 0.213 \times 10^{-3}$$

$$\gamma_{xy}^s = -\gamma_s/2.\ \cos 2\theta = 0.022 \times 10^{-3}$$

Inclusion of the irreversible fatigue strain is done in the manner of an offset strain:

$$\varepsilon_x^{fat} = \varepsilon_{c,2}^{fat}/2\ .\ (1-\cos 2\theta) = -6.09 \times 10^{-6}$$

$$\varepsilon_y^{fat} = \varepsilon_{c,2}^{fat}/2\ .\ (1+\cos 2\theta) = -7.50 \times 10^{-6}$$

$$\gamma_{xy}^{fat} = -\ \varepsilon_{c,2}^{fat}/2\ .\ \sin 2\theta = 13.5 \times 10^{-6}$$

Figure 3.1 (Box 5) - Material secant moduli:

The net strain values are estimated from Equation 2.8 (for concrete). The ratio of the average stress to the net strain gives the secant modulus for concrete. In the case of steel reinforcement, the ratio of the average stress in steel reinforcement to the induced strain gives the secant modulus.

E_{c1} = 480 MPa

E_{c2} = 15124 MPa

G_c = 466 MPa

E_{sx} = 200000 MPa

E_{sy} = 200000 MPa

Figure 3.1 (Box 6) - Material stiffness matrices [D_c], [D_s], [D]:

The stiffness matrices are estimated from Equations 3.4 to 3.8. The transformed composite stiffness matrix is obtained using Equation 3.9. The transformed composite stiffness matrix at 10000 cycles was obtained thus:

$$[D] = \begin{bmatrix} 7213 & 3367 & -3256 \\ 3367 & 6653 & -3992 \\ -3256 & -3992 & 3861 \end{bmatrix} \text{ (MPa)}$$

Figure 3.1 (Box 7) - Determine element prestress vector [σ^o]:

The element prestress vector was estimated from Equation 3.11. Herein, two prestrain values were considered: the shear strain at crack and the fatigue irreversible strain. The summation of the prestrains is equal to: $[\varepsilon_{ps}^{0}] = \begin{bmatrix} -0.22 \\ 0.21 \\ 3.58 \end{bmatrix}$ x 10^{-3} and,

$$[\sigma^{o}] = \begin{bmatrix} -0.13 \\ 0.26 \\ -5.35 \end{bmatrix} \text{MPa}$$

Figure 3.1 (Box 8) - Determine new estimates of strain $\{\varepsilon\}$, $\{\varepsilon_c\}$:

The total and net strain values are estimated using Equation 3.12. Since the results presented herein were obtained after convergence, the final values were also equal to the initial values. However, where significant variations are observed, the iteration continues as illustrated using the given steps. This procedure was repeated as the number of fatigue loading cycles was increased.

At the final collapse or failure of a structural element (in this case, the shear reinforcement in the vertical direction failed first), instability is observed and significant deformation persists. The results for the three different loads used are given in Figures 3.3 to 3.8. They are presented in terms of the crack slip evolution, shear stress evolution, reinforcement crack depth propagation (in the Y-direction where failure occurred), reinforcement strain, and stress evolutions.

The influence of fatigue load on the fatigue life is well-captured as observed in all deformation evolution plots (Figures 3.3 to 3.8). As the fatigue load increased, the corresponding fatigue life reduced, and the rates of deformation were observed to increase. In addition, the significance of the proposed approach stems from the fact that the profiles obtained in each case resemble the well-known fatigue deformation profile for reinforced concrete. Based on these observations, the deformation evolution within the cracked plane in reinforced concrete or steel fibre concrete can be obtained using the proposed approach.

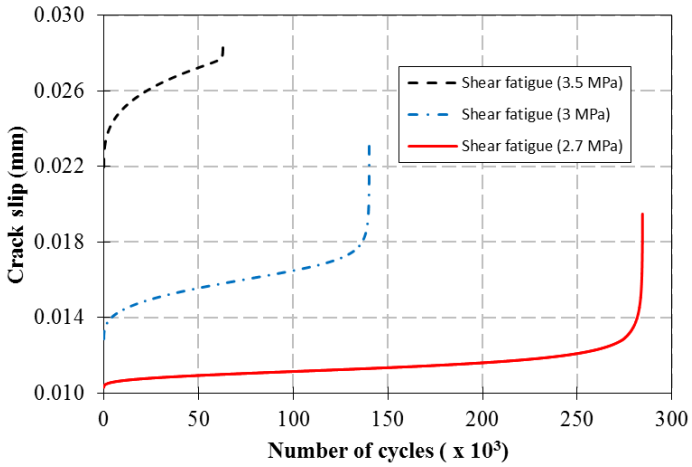

Fig. 3.3 - Crack slip evolution.

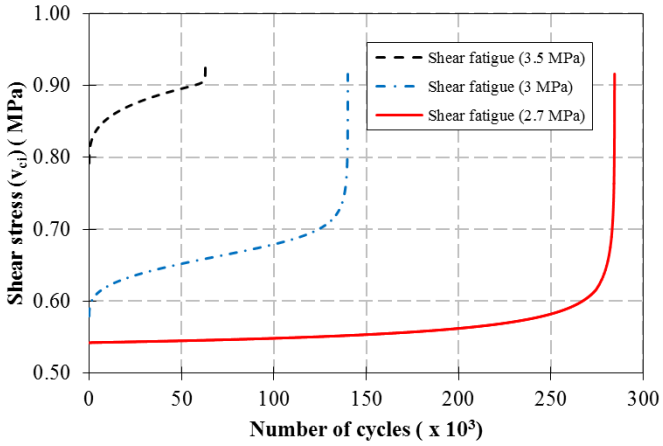

Fig. 3.4 - Shear stress evolution at crack.

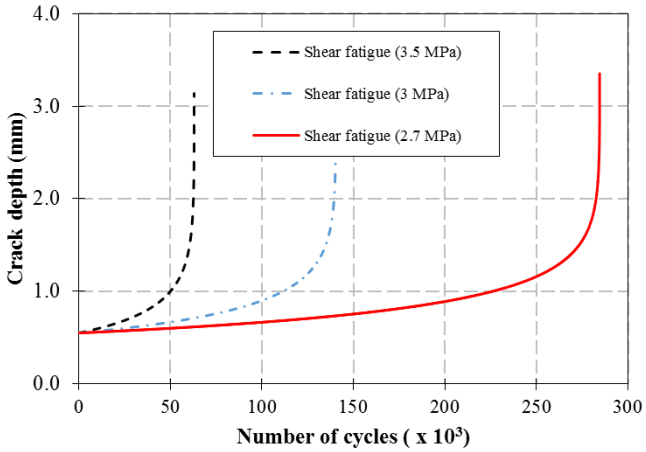

Fig. 3.5 - Reinforcement (Y-direction) crack growth depth.

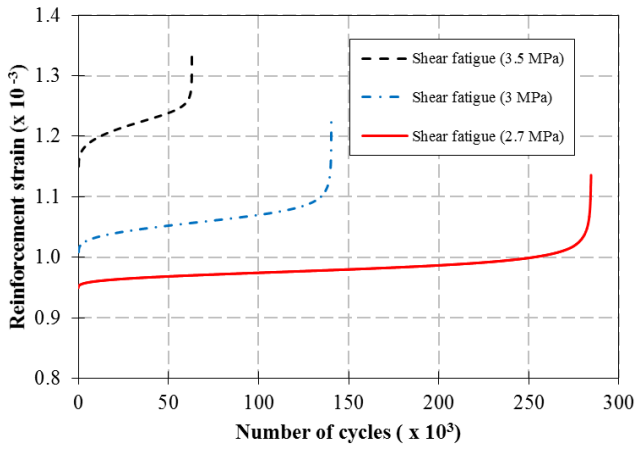

Fig. 3.6 - Reinforcement (X-direction) strain evolution at crack location.

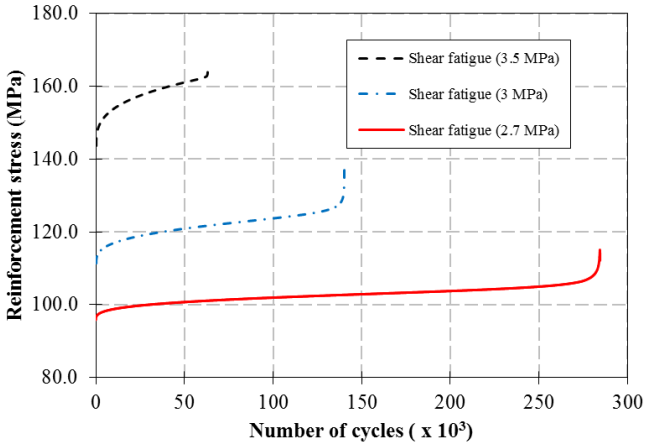

Fig. 3.7 - Reinforcement (X-direction) average stress evolution.

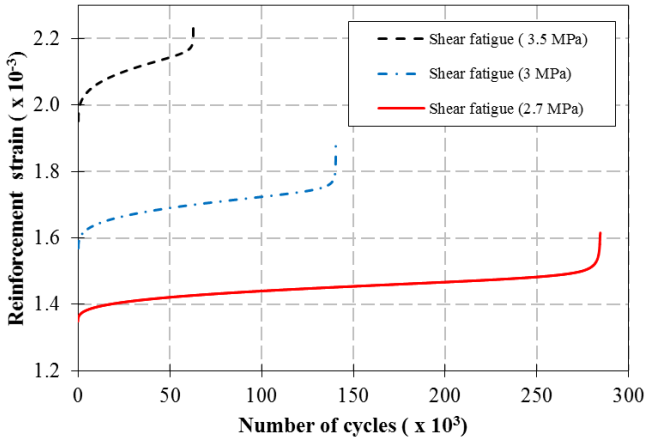

Fig. 3.8 - Localised reinforcement strain evolution (Y–direction).

CHAPTER 4: USE OF VecTor2 FOR FATIGUE DAMAGE ANALYSIS

VecTor2 nonlinear finite element analysis software was modified to account for fatigue damage analysis using the concepts described in the preceding Chapters. The approach for modelling of a structural element using Formworks is well documented in VecTor2 user's manual; however, this is reiterated alongside the new features for incorporating fatigue damage analysis.

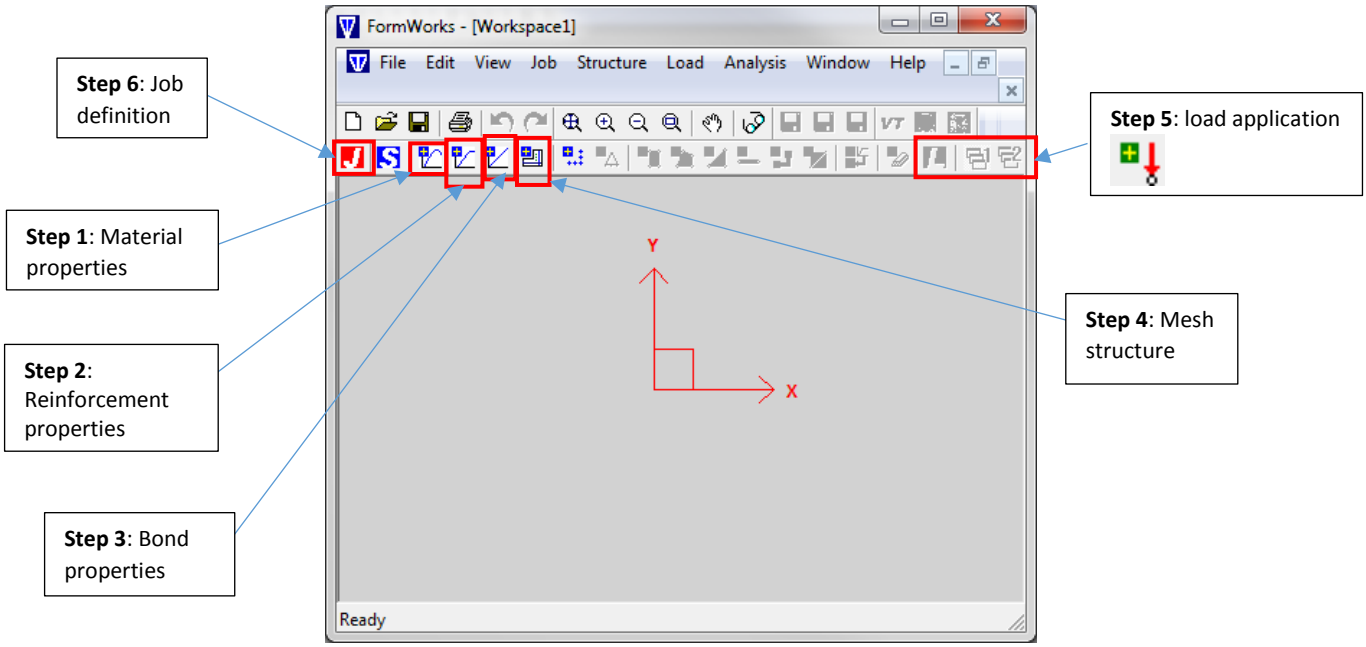

Figure 4.1- Formwork application window.

4.1 Defining Concrete Materials 

The icon above (pointed in step 1) is selected to input the material and geometrical properties for concrete such as thickness, compressive and tensile strengths, aggregate size, average crack spacing, etc. (Figure 4.2). For smeared reinforced concrete, the reinforcement component properties can also be included; however, the reference type box is used. For fatigue analysis, asides from steel fibre concrete, conventional reinforced concrete structural elements should be modelled using discrete reinforcement and the corresponding bond properties. For steel fibre-

reinforced concrete, other parameters for flexural strength (Model Code 2010) may be implemented within the smeared reinforcement properties.

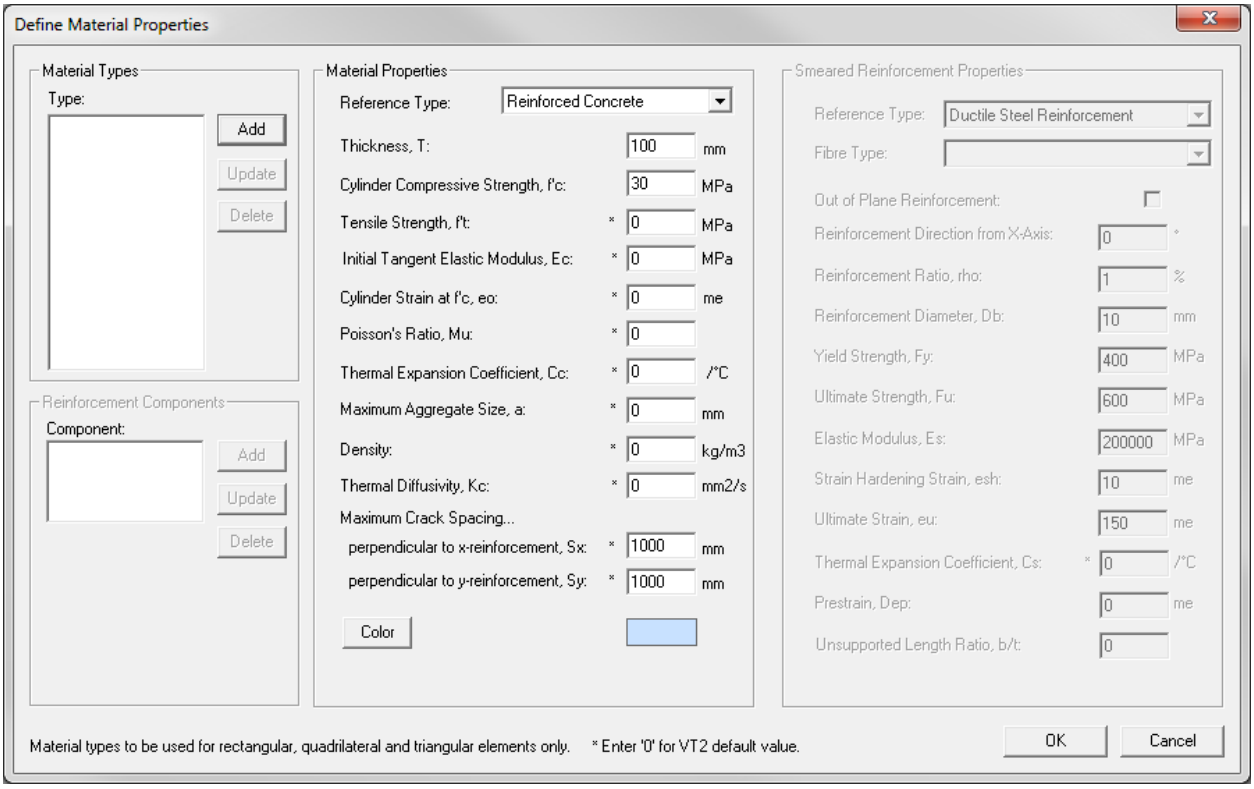

Figure 4.2 – Reinforced concrete materials properties dialog box.

4.2 Defining Reinforcement Properties

For high-cycle fatigue life prediction, fracture of reinforcing steel or structural collapse is assumed to be brittle. As such, yielding of steel reinforcement coincides with fatigue failure. The reinforcement properties (Figure 4.3) in the **Define Reinforcement Materials** dialog box are selected such that the strain-hardening of steel reinforcement is neglected. The ultimate yield strength of the selected ductile steel reinforcement should have the same value as the yield strength (variation of about 1% at most). Other corresponding properties such as cross-section area, reinforcement diameter, elastic modulus etc. are also required.

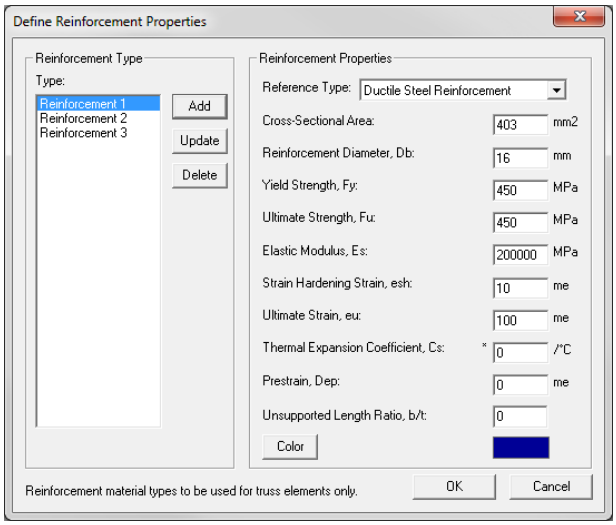

Fig. 4.3 – Reinforcement materials dialog box.

4.3 Bond Types

As described in VecTor2 user's manual for bond stress-slip relationships between concrete and discrete reinforcement under different loading conditions, the reference type of steel bars, the bond properties, bar clear cover, number of reinforcement layers for embedded bars, etc. are selected (mainly embedded deformed bars) as shown in Figure 4.4.

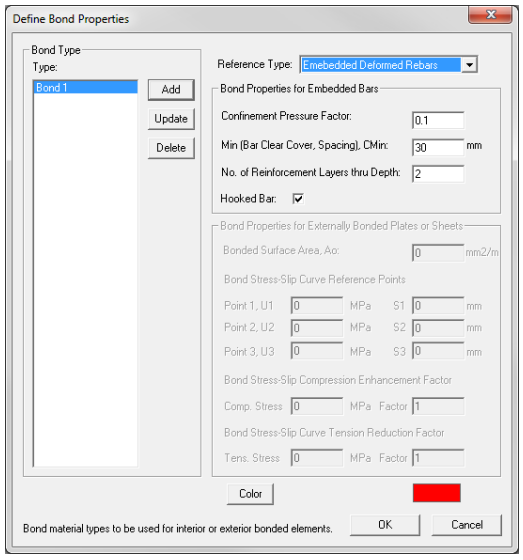

Figure 4.4 – Bond properties dialogue box.

4.4 Structure and Mesh Definition 

The creation of the element or concrete regions, inclusion of discrete steel reinforcement, inclusion of attributes such as bond type, discretization and mesh type, indication of constraints, and meshing, are well illustrated in VecTor2 user's manual. This is indicated as step 4 in Figure 4.1.

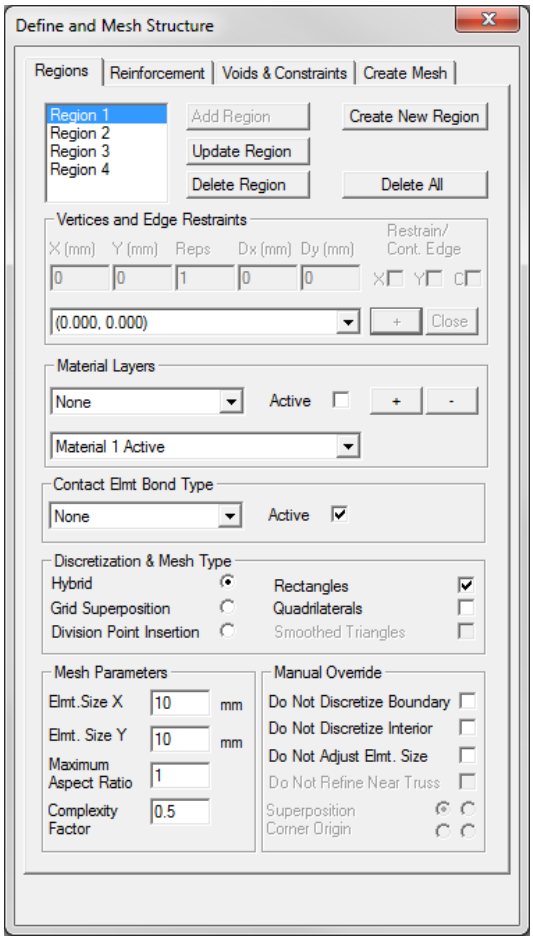

Figure 4.5 – structure and mesh definition.

4.5 Load Application under Fatigue Loading 

A fatigue waveform is shown in Figure 4.6, with the indication of the maximum and the minimum fatigue loads. Basically, the maximum fatigue load is required for loading in VecTor2. However,

the effect of the minimum fatigue loading in high-cycle fatigue is accounted for using the load ratio R ($\frac{F_{min}}{F_{max}}$). (Note: this is indicated as step 5 in Figure 4.1).

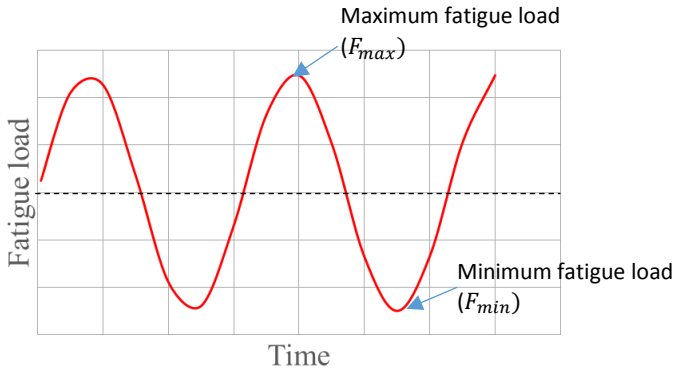

Fig. 4.6 – Fatigue load wave form (sinusoidal)

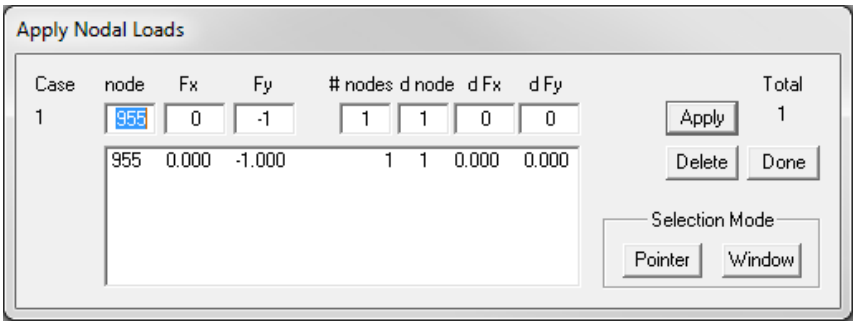

Figure 4.7 – Load application

The direction of the maximum load is considered by indicating a negative sign for a vertical force acting downwards. In addition, a unit load is indicated at the corresponding node where the fatigue load acts. The concept of load factor will be discussed subsequently.

4.6 Job Definition

The implementation of fatigue parameters is considered within the **Define job dialog box**. The procedure for appropriate model selection is illustrated thus

In the **Define job dialog box** (Figure 4.8), the first box corresponds to the job control. Herein, the maximum fatigue load is entered as the **initial factor**, while a reasonable increment (usually 0.5

or 1.0) is also typed in the box for the **incremental factor**. All other parameters may be selected as described in VecTor2 user's manual.

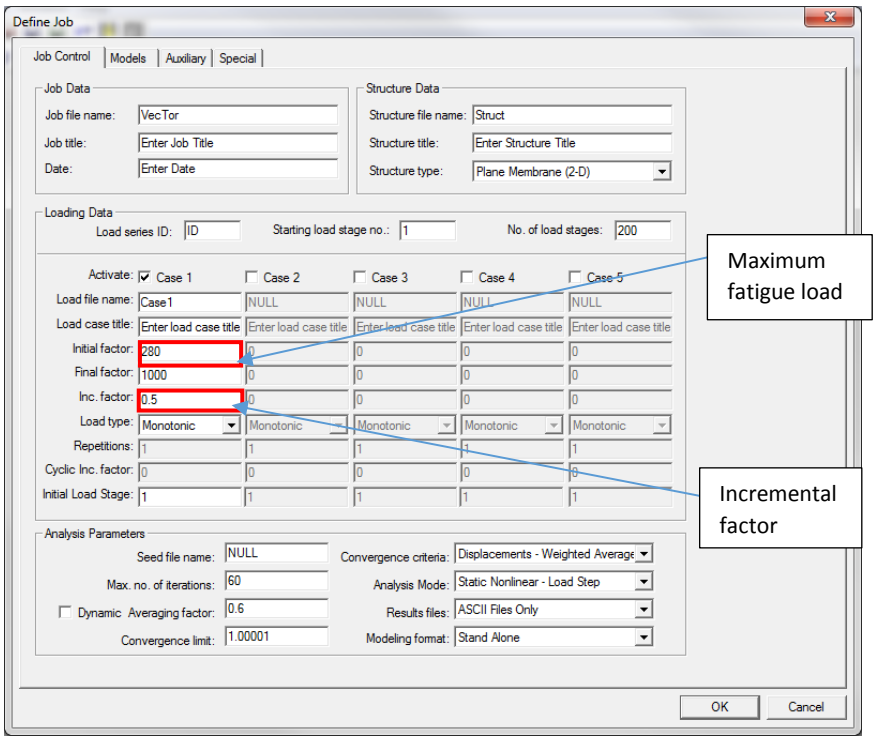

Figure 4.8 – Job control.

The models to be used are obtained by clicking on the **Models** button in the **Define job** dialog box. Under fatigue loading for concrete material, the Hognestad's equation or Popovics' equation for compression can be used depending on the type of concrete (normal or high strength, respectively). For the normal strength-compression post-peak, the modified Park-Kent is used, while the Popovics/Mander model is used for the high strength concrete compression post-peak. Asides the compression pre-peak and Post-peak models, other models required are similar for normal and high strength concrete (default values are recommended). These are shown in Figure 4.9 for high-strength plain concrete.

In the case of steel fibre-reinforced concrete, **Lee et al. (2011) FRC models** are used. For compression softening, the **Vecchio 1992-A (e1/e2) model** is recommended, while the **Advanced Lee (2009) model** is suggested for crack stress calculation. Further, **Vecchio and Lai's model** is recommended for the crack slip calculation, the **Lee 2010 (w/post-yield) model** is suggested for tension stiffening, and the **FIB model code 2010** is used for tension softening. The reinforcement models are left as default.

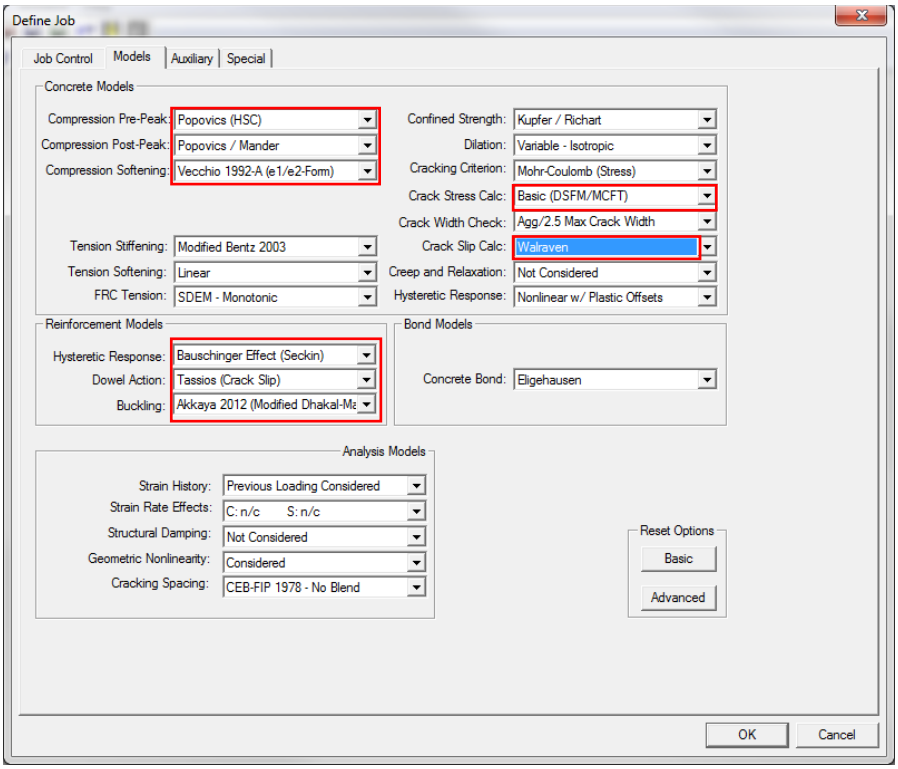

Fig. 4.9 – Concrete models

4.7 Defining Fatigue Loading Parameters in Job

In the Job dialog box, select **special**.

Select **Considered** within the tray corresponding to **Concrete/Reinf. Fatigue** (Figure 4.10).

Click on **Show Fatigue Parameters (Figure 4.11)**. The boxes are filled appropriately with values for frequency (in Hertz), loading ratio (R), fatigue wave-form, permissible error (0.01 default),

and interval of loading cycles. The number of fatigue loading cycles is increased for each analysis conducted. Basically, the load-deformation plot is obtained for different loading cycles. As the number of cycles included increases, the load capacity reduces and the deformation increases. An instance is reached when the load capacity is approximately equal to the **fatigue load** (used as the initial factor in Figure 4.8). The corresponding number of cycles is the fatigue life.

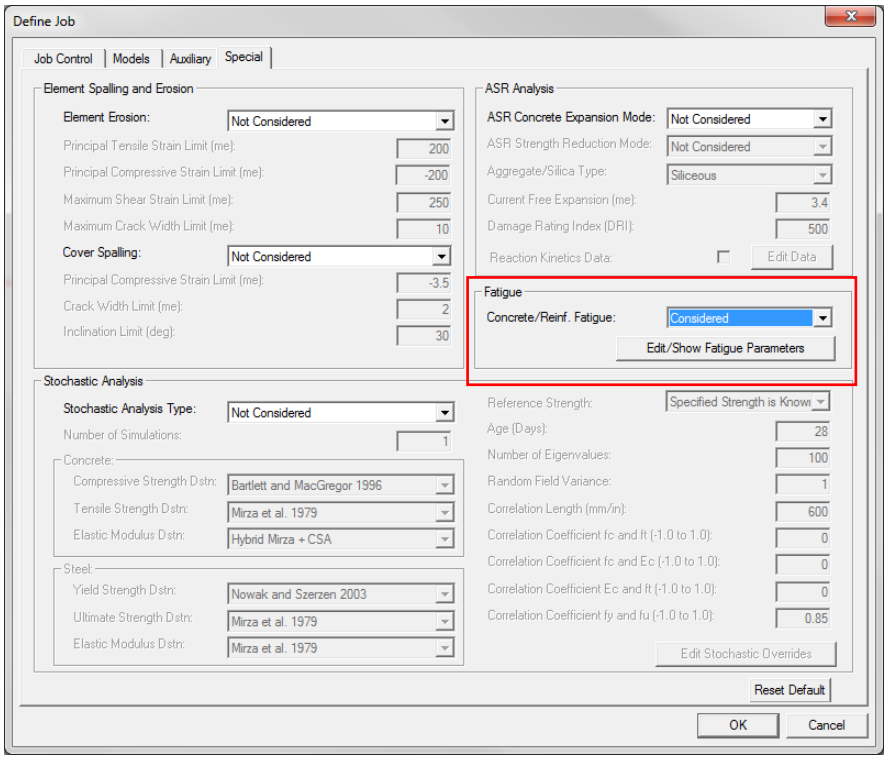

4.10 – Fatigue damage consideration

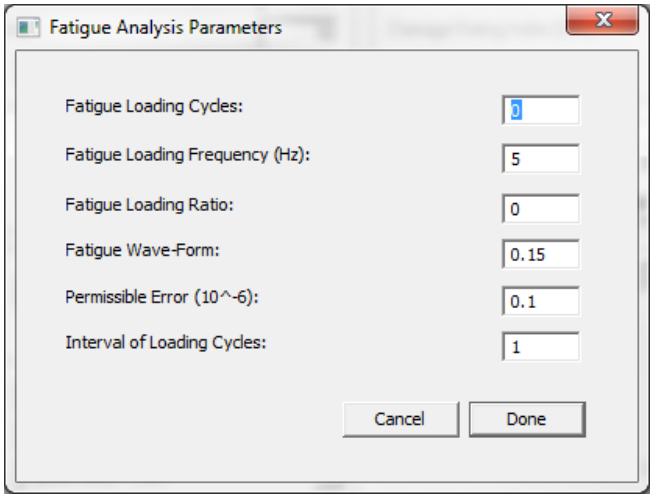

Fig. 4.11 – Fatigue damage parameters

For reduced analysis time, a reasonable interval should be chosen for the fatigue analysis. For example, the ratio of the selected number of cycles to the interval of loading cycles may be taken as 100 or 1000.

4.8 Solved example

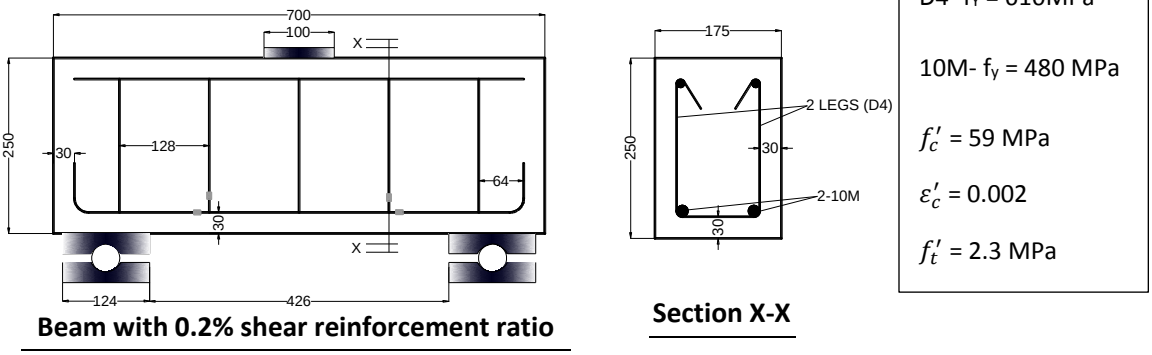

Fig. 4.12 - Details of deep beam specimen.

The solution to the fatigue life prediction of the beam given in Figure 4.12 using Formworks modelling procedure/VecTor2 analysis is presented. Herein, the fatigue life of the beam when subjected to a fatigue load of 80% of the ultimate load is considered (Figure 4.13). From an initial monotonic load-deformation response without fatigue damage, an ultimate load capacity value of 245 kN was obtained from the model (Figure 4.14); hence, 80% of the capacity is equal to 196 kN.

This value corresponds to the maximum fatigue load to be used. The loading frequency was assumed to be 5 Hz, while the fatigue loading ratio and fatigue waveform were assumed to be zero and 0.15 (sinusoidal wave), respectively. The residual capacities which correspond to different fatigue loading cycles are shown in Figure 4.15. As observed, at 40 000 cycles, the loading cycles was approximately close to the applied fatigue load; hence, its failure instance. The mid-span deflection evolution is also given in Figure 4.16. Towards failure, the rate of increase was higher.

Other results such as reinforcement stresses or strains as the loading cycles increase can also be obtained. As indicated initially, structural failure due to high-cycle fatigue loading will occur when the reinforcing bars fracture (Figure 4.17). This corresponds to the yield value of the reinforcement. As shown in Figure 4.17, the shear reinforcement did not fracture; rather, collapse was a result of the longitudinal reinforcement stress reaching the yield value (max stress in reinforcement at 40 000 cycles corresponds to the yield value of 480 MPa – Figure 4.12).

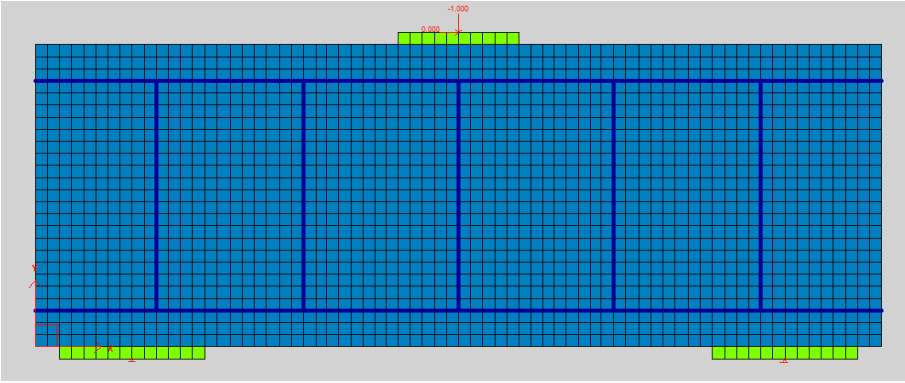

Fig. 4.13 – Finite element mesh for beam.

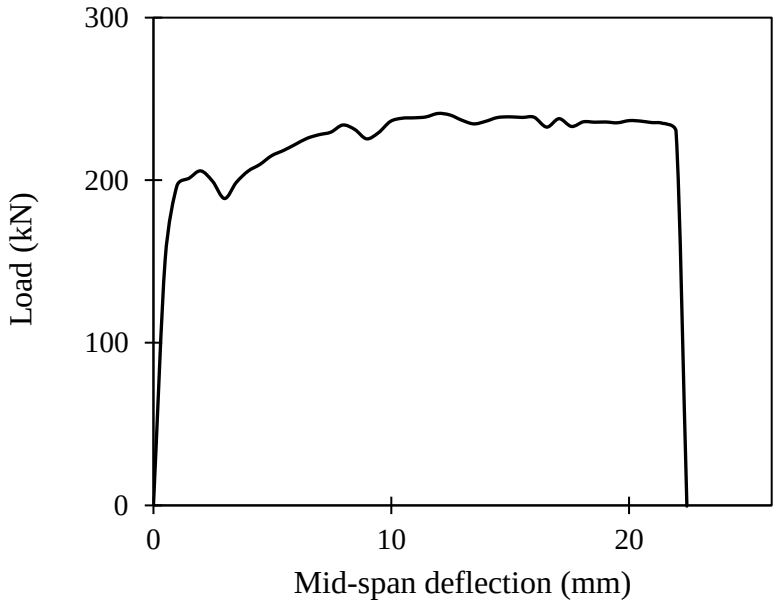

Fig. 4.14 – Load versus mid-span deflection.

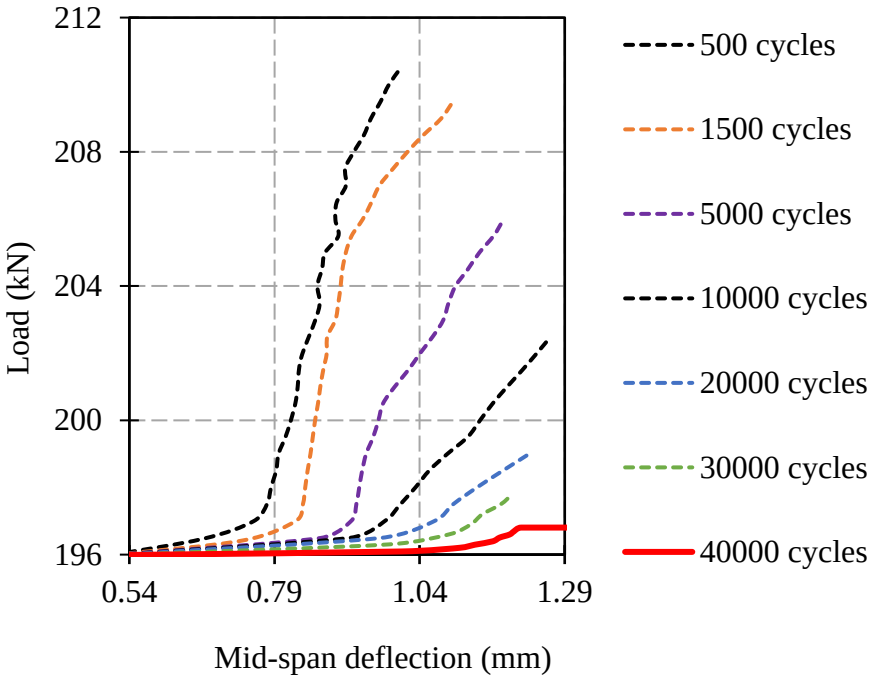

Fig. 4.15 – Fatigue residual capacity.

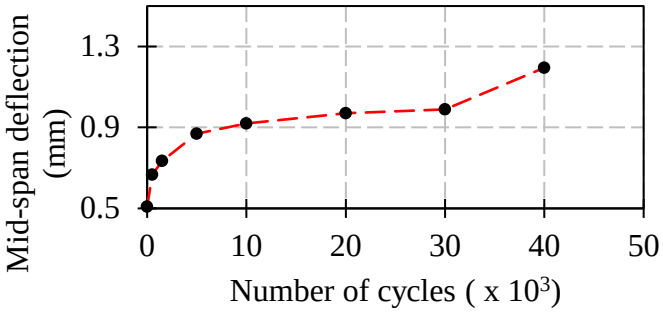

Fig. 4.16 – Mid-span deflection evolution.

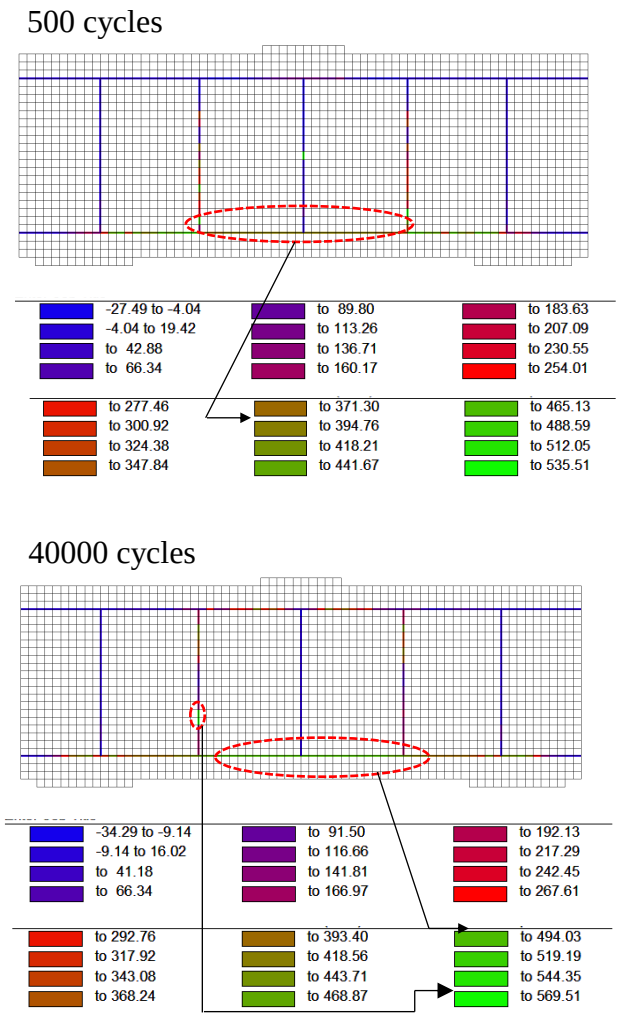

Fig. 4.17 – Evolution of stresses in reinforcing bars (stresses shown in MPa).

5.0 SUMMARY AND RECOMMENDATION

5.1 Summary

An approach which can be used to predict the fatigue life of a reinforced concrete structural element using VecTor2 was illustrated. The analysis was based on the implementation of fatigue damage mechanisms in concrete and steel reinforcement, especially at the cracked concrete plane. The founding principle (for appropriately reinforced concrete elements) assumes that the fatigue life corresponds to the instance at which the fatigue residual capacity becomes equal to the fatigue load applied. This has been shown to be realistic based on validation of experimental investigations with finite element analysis using the proposed approach.

5.2 Recommendation

Depending on the complexity of the structural element and the density of embedded reinforcement, certain anomalies may occur while modelling. For ease, reasonable interval of fatigue loading cycles and load increments should be used at intervals especially at instances when the degradation becomes significant. The use of an elastic-perfectly plastic model for steel reinforcement is reiterated and strongly encouraged, as this dictates the fatigue residual capacity. Since high-cycle fatigue is brittle in nature, the increased strain values in steel reinforcement due to crack growth should not take into account the strain hardening effects. This obviously accounts for the substantial increase in reinforcement temperature as cracks propagate.

6.0 REFERENCES

Amir et al. (2012). “Fatigue Performance of High-Strength Reinforcing Steel.” Journal of Bridge Engineering, Vol. 17, No. 3, pp. 454-461.

British Standard (2005). “Guide to Methods for Assessing the Acceptability of Flaws in Metallic Structures.” BS 7910.

Collins, M.P., Mitchell, D. (1997). “Prestressed Concrete Structures.” Response Publications, Canada, 766 pp.

Cook D.J., and Chindaprasirt P. (1980). “Influence of Loading History upon the Compressive Properties of Concrete.” Magazine of Concrete Research, Vol. 32, No. 111, 1980, pp. 89-100.

Deluce, J.R., Lee, S.C, and Vecchio, F. (2014). “Crack Model for Steel Fibre-Reinforced Concrete Members Containing Conventional Reinfocement.” ACI Structural Journal, Vol. 111, No. 1, pp. 93-102.

Dowling, N.E. 1993. Mechanical Behaviour of Materials, Prentice Hall, New Jersey.

Edalatmanesh R., and Newhook J.P. (2013). “Residual Strength of Precast Steel-Free Panels.” ACI Structural Journal, Vol.110, pp. 715-722.

Isojeh, B., El-Zeghayar, M., and Vecchio, F.J. (2017a). “ Concrete Damage under Fatigue Loading in Uniaxial Compression.” ACI Materials Journal, Vol. 114, No. 2, pp. 225-235.

Isojeh, B., El-Zeghayar, M., and Vecchio, F.J. (2017b). “ Simplified Constitutive Model for Fatigue Behaviour of Concrete in Compression.” Journal of Materials in Civil Engineering, DOI: 10.1061/(ASCE)MT.1943-5533.0001863.

Gao L., and Hsu C.T.T. (1998). “Fatigue of Concrete under Uniaxial Compression Cyclic Loading.” ACI Materials Journal, Vol. 95, No. 5, pp. 575-581.

Herwig A. (2008). “Reinforced Concrete Bridges under Increased Railway Traffic Loads-Fatigue Behaviour and Safety Measures.” Ph. D Thesis No. 4010, Ecole Polytechnique Federale de Lausanne.

Hirt, M.A., Nussbaumer, A. 2006. Construction metallique: notions fondamentales et methods de dimensionnement, nouvelle edition revue et adaptee aux nouvelles norms de structures. Traite de Genie Civil de l’Ecole Polytechnique Federale, Vol. 10. Lausanne, Switzerland.

Holmen J.O. (1982). “Fatigue of Concrete by Constant and Variable Amplitude Loading.” ACI SP Vol. 75, No. 4, pp. 71-110.

Isojeh, B., El-Zeghayar, M., and Vecchio, F.J. (2017c). “ Fatigue Behaviour of Steel Fibre Concrete in Direct Tension.” Journal of Materials in Civil Engineering, DOI: 10.1061/(ASCE)MT.1943-5533.0001949.

Isojeh B., El-Zeghayar M., Vecchio, F.J. “Fatigue Resistance of Steel-Fibre Reinforced Concrete Deep Beams.” ACI Structural Journal, Vol. 114, No. 5, pp. 1215-1226.

Isojeh B., El-Zeghayar M., Vecchio, F.J. (2017e). “High-Cycle Fatigue Life Prediction of Reinforced Concrete Deep Beams.” Engineering Structures Journal, Vol. 150, pp. 12-24.

Isojeh, M.B., and Vecchio, F.J (2016). “Parametric Damage of Concrete under High-Cycle Fatigue Loading in Compression.” Proc., 9th International Conference on Fracture mechanics of Concrete and Concrete Structures. FraMCoS-9 2016; 10.21012/FC9.009.

Lee, S.C., Cho, J.Y., Vecchio, F.J. (2016). “Analysis of Steel Fibre-Reinforced Concrete Elements Subjected to Shear.” ACI Structural Jorunal, Vol. 113, No. 2, pp. 275-285.

Paris, P., Gomez, M.P., and Anderson W.E. (1961). “A Rational Analytical Theory of Fatigue.” The Trend in Engineering, Vol. 13, pp. 9-14.

Rocha M., and Bruhwiler E. (2012). “Prediction of Fatigue Life of Reinforced Concrete Bridges.” In Biondini and Frangopol (Eds) Bridge Maintenance, Safety, Management, Resilience and Sustainability, pp. 3755-3760.

Schaff J.R., and Davidson B.D. (1997). “Life Prediction Methodology for Composite Structures. Part 1- Constant Amplitude and Two-Stress Level Fatigue.” Journal of Composite Materials, Vol. 31, No. 2, pp. 128-157.

Vecchio F.J. (2000). “Disturbed Stress Field Model for Reinforced Concrete: Formulation.” Journal of Structural Engineering, Vol. 127, No. 1, pp. 1070-1077

Vecchio F.J. (2001). “Disturbed Stress Field Model for Reinforced Concrete: Implementation.” Journal of Structural Engineering, Vol. 127, No. 1, pp. 12- 20.

Vecchio, F.J., Lai, D., Shim, W., Ng, J. (2001). “Disturbed Stress Field Model for Reinforced Concrete: Validation.” Journal of Structural Engineering, Vol. 127, No. 4, pp. 350-358.

Zhang B., Phillips D.V., and Wu K. (1996). “Effects of Loading Frequency and Stress Reversal on Fatigue Life of Plain Concrete.” Magazine of Concrete Research, Vol. 48, pp. 361-375.